Taylor & Francis
Taylor & Francis Group

Transportmetrica A: Transport Scie

ISSN: (Print) (Online) Journal homepage: https://www.tandfonline.com/loi/ttra21

FMS-dispatch: a fast maximum s policy for shared autonomous v exiting passengers under stoch demand

Te Xu, Maria Cieniawski & Michael W. Levin

TRANSPORTMETRICA A: TRANSPORT SCIENCE
https://doi.org/10.1080/23249935.2023.2214968

Taylor & Francis
Taylor & Francis Group

FMS-dispatch: a fast maximum stability dispatch policy for shared autonomous vehicles including exiting passengers under stochastic travel demand

Te Xu[a,b], Maria Cieniawski[a] and Michael W. Levin[a]

[a]Department of Civil, Environmental and Geo-Engineering, University of Minnesota, Minneapolis, MN, USA; [b]Department of Industrial and Systems Engineering, University of Minnesota, Minneapolis, MN, USA

ABSTRACT

Shared autonomous vehicles (SAVs) are a fleet of autonomous taxis that provide point-to-point transportation services for travellers, and have the potential to reshape the nature of the transportation market in terms of operational costs, environmental outcomes, increased tolling efficiency, etc. However, the number of waiting passengers could become arbitrarily large when the fleet size is too small for travel demand, which could cause an unstable network. An unstable network will make passengers impatient and some people will choose some other alternative travel modes, such as metro or bus. To achieve stable and reliable SAV services, this study designs a dynamic queueing model for waiting passengers and provides a fast maximum stability dispatch policy for SAVs when the average number of waiting for passengers is bounded in expectation, which is analytically proven by the Lyapunov drift techniques. After that, we expand the stability proof to a more realistic scenario accounting for the existence of exiting passengers. Unlike previous work, this study considers exiting passengers in stability analyses for the first time. Moreover, the maximum stability of the network doesn't require a planning horizon based on the proposed dispatch policy. The simulation results show that the proposed dispatch policy can ensure the waiting queues and the number of exiting passengers remain bound in several experimental settings.

ARTICLE HISTORY
Received 11 August 2022
Accepted 12 May 2023

KEYWORDS
Shared autonomous vehicles; Lyapunov drift techniques; maximum stability; dispatch policy; exiting passengers

1. Introduction

With the combination of shared mobility-on-demand service and vehicle connection and automation (Tu et al. 2019; Ma, Wang, and Ruan 2021; Ma et al. 2022; Zhou et al. 2021), a new travel mode choice of shared autonomous vehicles (SAVs), also known as automated mobility-on-demand or shared autonomous vehicles' mobility service, may reshape the transportation market (Fagnant and Kockelman 2014; Fagnant, Kockelman, and Bansal 2015; Fagnant and Kockelman 2015; Boesch, Ciari, and Axhausen 2016; Hyland and Mahmassani 2017). Specifically, an SAV service is a fleet of autonomous taxis that provide

CONTACT Te Xu te000002@umn.edu Department of Civil, Environmental, and Geo-Engineering, 500 Pillsbury Drive S.E., Minneapolis, MN 55455; Department of Industrial and Systems Engineering, 207 Church Street SE, Minneapolis, MN, USA 55455

point-to-point transportation services for travellers. Researchers have found that SAVs may be beneficial to society in terms of operational cost, environment, policies, tolling, etc. For example, Fagnant and Kockelman (2014) and Fagnant, Kockelman, and Bansal (2015) found that SAVs could reduce the usage of private vehicles significantly. Specifically, they predicted that one SAV would replace 11 privately-owned vehicles. The reduction in private car usage can have significant environmental benefits. For governments, SAVs are beneficial to road-tolling system operations (Narayanan, Chaniotakis, and Antoniou 2020). From the supply side, SAVs are also beneficial to the implementation of transportation management policies like parking management (Zhang and Guhathakurta 2017) and intersection management (Chen et al. 2020). For individuals, SAVs may become highly competitive with traditional car ownership when considering the long-term cost (Hörl et al. 2019). Overall, based on the past literature, SAVs would enable future transportation systems to have higher safety (Fagnant and Kockelman 2015; Teoh and Kidd 2017) and reduced emissions (Greenblatt and Saxena 2015; Lokhandwala and Cai 2018).

In reality, the number of waiting travellers is uncertain and stochastic. If the fleet size is too small for travel demand, some passengers would be unserved. That would cause the number of waiting passengers to become arbitrarily large, which we call an unstable network. In other words, stability means that all passengers are served. Moreover, as travel time is the chief concern for passenger mode of choice, if SAV queues grow longer than alternative travel modes such as transit, taxi, or walking, people are more likely to use those alternates than SAVs. Therefore, unstable and unreliable SAV services cannot maximise the benefits of SAVs (Li et al. 2021). Thus, the stability of transportation systems is a topic worthy of attention. The first paper discussing stability is developed for scheduling communication and power network (Tassiulas and Ephremides 1990). To achieve transportation network stability, Varaiya (2013) proposed a max-pressure traffic signal control policy and proved their policy could achieve network stability whenever possible. Further studies based on Varaiya (2013)'s max-pressure control have received growing attention due to its advantages, such as maximising passenger throughput without requiring arrival rates (Levin, Hu, and Odell 2020; Xu et al. 2022; Xu, Bika, Levin n.d. a). These properties of max-pressure control could be useful for SAV systems since we want to minimise the queue length of passenger queues and provide stable service for travellers.

Inspired by max-pressure policies, this study successfully develops a fast maximum stability dispatch policy for SAVs. Although some studies have included ride-sharing (Farhan and Chen 2018; Gurumurthy, Kockelman, and Simoni 2019; Hyland and Mahmassani 2020), which can be defined as driving multiple passengers with near origins, destinations and similar departure times, or electric SAVs and charging behaviours (Loeb and Kockelman 2019; Chen and Kockelman 2016; Li et al. 2021), or dynamic rebalancing (Zhang and Pavone 2016), we do not include these behaviours in this study due to the analytical complexity of our presented work. Our results focus on an analytical dispatch method for SAVs without ride-sharing, and we hope these results will be extended to ride-sharing in the future.

Our research is focussed on queue length stability for waiting passengers. The practical meaning of 'stability' in the paper is that the passenger demand rate is the same as the SAV service rate, and then the passenger waiting queue length will not grow up as time goes on. Li et al. (2021), Kang and Levin (2021), and Levin (2022) are the only three studies on the stability of passenger queues for SAVs. Li et al. (2021) defined the nodes as SAVs and

passengers and proposed a minimum drift plus penalty approach for SAEV systems that can ensure the stability of customer waiting time and vehicle dispatching cost can be controlled. Although they analytically proved the stability of the SAEV systems, they did not characterise the stable region with specific mathematical equations, which prevents accurately obtaining the maximum stable trips under a given fleet size. Note that Li et al. (2021) use waiting time as the state, instead of the size of the waiting queue, and they also prove stability for any arrival rate in the stable region. The reason we use the passengers' waiting queue length as the state is that we want to characterise the stable region with specific mathematical equations, which give the set of passengers' travel demands that can be served by a given SAVs fleet size, and find a dispatch policy that can make SAVs serve any demand in the stable region. When demand is in the stable region, we can analytically prove the stability of our dispatch policy and find the solution of maximum stable trips per hour under a given fleet size. Kang and Levin (2021) used a similar queueing model waiting for passengers and characterise the stable region, but their maximum-stability dispatch policy requires a time horizon to achieve stability, which takes much more computation time. Later on, Levin (2022) proposed a general maximum-stability dispatch policy for SAV dispatch, which considered a general class of SAV behaviours such as ridesharing, charging, and integration with public transit and characterise the maximum throughput. Furthermore, Levin (2022) used waiting time as the state, which is the same as Li et al. (2021). None of the previous studies considered the possibility of waiting for passengers to leave the waiting queues due to the complexity of the stability proof and simulation.

The contributions of this paper are as follows: (1) We design a dynamic queuing model for waiting passengers that considers the possibility of exiting passengers for the first time. (2) We leverage a policy for stabilising the transportation network under stochastic travel demand. (3) The assignment method calculates the optimal dispatch policy for which SAVs in the network are assigned to the matching passengers in the network. (4) We analytically characterise the stable region or the sets of demand that could be served by any dispatch policy. Then, we analyse the stability when demand is within and outside the stable region when the proposed dispatch policy is used. (5) We prove the proposed fast maximum stability dispatch policy can stabilise the network when the average waiting passenger is bound in expectation based on Lyapunov drift techniques. (6) We extend the proposed policy to a more realistic scenario, considering the possibility of exiting passengers for the first time, and prove the proposed dispatch policy can still achieve maximum stability using Lyapunov drift techniques. (7) Finally, we test the performance of proposed SAV dispatch policies in simulation.

The remainder of this paper is organised as follows: Section 2 summarises the relevant literature about SAVs, such as agent-based simulation and optimal dispatch algorithms. Section 3 introduces the stability analysis used to determine the queuing model on the network. Section 4 extends this model to consider exiting passengers in the queuing model and proves that the maximum-stability policy is still valid when some passengers exit the queues. Section 5 presents the simulation results, and we conclude in Section 6.

2. Literature review

The dispatch model in this work is mainly inspired by the shared autonomous vehicle-to-customer assignment problem. In this part, we first review related papers focussing

on shared autonomous vehicles. Then we review the existing literature on max-pressure control.

2.1. Shared autonomous vehicles

The mobility-on-demand system has emerged as a new competitive mode choice for passengers around the world. Companies such as DiDi Chuxing in China, Uber, and Lyft in the United States have been widely used (Wang and Yang 2019; Liu et al. 2022). Wang and Yang (2019) provided a general framework for understanding interactions between the demand and supply side of ride-sourcing systems. With the rapid development and popularisation of autonomous vehicles, SAVs may reshape the existing urban transportation system (Becker and Axhausen 2017; Hyland and Mahmassani 2017; Mourad, Puchinger, and Chu 2019; Narayanan, Chaniotakis, and Antoniou 2020). Over the past few years, researchers began to focus on the new trend of shared autonomous vehicles from the perspectives of transportation environment and sustainability, transportation economy, traffic policies, mode choice preference, traffic supply and demand, and so on. Narayanan, Chaniotakis, and Antoniou (2020) and Golbabaei, Yigitcanlar, and Bunker (2020) present literature surveys of SAVs. Generally, SAV modelling problems can be characterised as optimal SAV dispatch problems and agent-based simulation problems (Levin 2022).

The optimal SAV dispatch problem is a well-studied topic in the realm of the vehicle routeing problem. The optimal SAV dispatch problem is to find the optimal assignment of SAVs to passengers. These studies used optimisation techniques on the problem structure to improve performance. Some researchers proposed simplistic first-come-first-serve (FCFS) methods to assign travellers to the nearest idle SAVs (Fagnant, Kockelman, and Bansal 2015; Chen, Kockelman, and Hanna 2016). Several researchers split the city into multiple service regions and then assigned the waiting passengers to the nearest idle SAVs in their waiting sub-region. However, the simplified nearest dispatch or assignment may not achieve optimal results for passenger waiting time and SAV travel times. To improve the operational performance of shared autonomous vehicle services and reduce operational costs, some researchers applied mathematical programming to the SAVs dispatch or assignment problem. Hanna et al. (2016) applied the collision-avoiding role assignment with minimal-makespan (SCRAM) for matching vehicles and passengers and then dispatch the matching vehicles to pick up waiting for customers. After comparing the four algorithms, SCRAM could reduce the variance in the waiting time of passengers by producing a fair assignment. Hyland and Mahmassani (2018) compared a SAV service system with no shared rides by two first-come-first-served vehicle dispatching strategies and four optimisation-based strategies, and found that the strategies that divert dispatching when new traveller requests appear would have better results when the SAV fleet size is small. But when the SAV fleet size increased, the simple first-come-first-served strategies could become more competitive with advanced optimisation-based approaches. Model predictive control is another modelling method in optimal SAV dispatching problems (Zhang and Pavone 2016; Zhang, Rossi, and Pavone 2016). Yu et al. (2022) presented an integrated optimisation framework for locating depots in a SAV systems under demand uncertainty.

Recently, user equilibrium, competition between human-driven vehicles, mixed-fleet size, and electrification were included in SAV optimal matching and routeing problems (Ge, Han, and Liu 2021). Specifically, Ge, Han, and Liu (2021) constructed a bi-level problem,

where the upper-level is a matching and routeing problem and the lower level involves a user equilibrium among conventional vehicles. Guo, Chen, and Liu (2022) proposed a time-space network flow model to optimise SAV dispatch and relocation when mode choices between SAVs and human-driven private vehicles are considered. Santos and de Almeida Correia (2021) proposed a flow-based integer programming approach to optimise the fleet size and SAV movements. The fleet size in their research was combined with cars, minibuses, or a mixed fleet of both. Boewing et al. (2020) presented a mixed-integer programme to optimise vehicle coordination and charge scheduling problems into mobility-on-demand systems with electrical autonomous taxis.

Agent-based simulation is another approach to studying SAV performance (Khan and Habib 2023; Poulhès and Berrada 2020). Fagnant and Kockelman (2014) used an agent-based model to simulate the potential travel and environmental influences of SAVs after more than one hundred days in a grid-based city. The simulation results show that one SAV would replace 11 private vehicles. Since ride-sharing has been proven to provide more benefits for taxi services (Vazifeh et al. 2018), many researchers find that ride-sharing applications in SAVs could bring further benefits to the SAV system. To better understand the ride-sharing implementation with SAVs, Fagnant and Kockelman (2018) and Gurumurthy, Kockelman, and Simoni (2019) used MATsim, an agent-based simulation tool to test the operation of SAVs by enabling dynamic ride-sharing in Austin, Texas, and found that dynamic ride-sharing could reduce the average service time. Hyland and Mahmassani (2018, 2020) used an agent-based model to compare the SAV system with and without ride-sharing. The results showed that ride-sharing with SAVs could reduce traveller's waiting time and vehicle kilometres travelled (VKT) while using a smaller fleet size to provide the same level of service. Furthermore, Hyland and Mahmassani (2020) also found that ride-sharing could provide the same level of service by operating smaller fleet sizes of SAVs and even reduce the congestion, emission, and energy consumption. Gurumurthy and Kockelman (2020) analysed Americans' preferences for dynamic ride-sharing with SAVs, and found that Americans expect much of their long-distance travel (for trips over 50 miles, one-way) to shift towards AVs and SAVs. Overall, shared autonomous vehicles have great impacts on the environment regarding emissions and energy consumption. The reduced fleet size of SAVs could further reduce CO_2 emissions (Greenblatt and Saxena 2015; Martinez and Viegas 2017; Lokhandwala and Cai 2018). Some researchers have predicted that SAVs will use electric vehicles to reduce vehicle emissions, and they extended agent-based models to study the charging and energy consumption of shared autonomous electrical vehicles (Chen, Kockelman, and Hanna 2016; Loeb, Kockelman, and Liu 2018; Farhan and Chen 2018; Zhang and Chen 2020; Becker et al. 2020; Liang et al. 2023). Some studies used agent-based simulation to study the SAV system performance after integrating with public transit (Huang, Kockelman, and Garikapati 2022).

Previous studies gave limited attention to the stability of SAV systems and cannot guarantee the long-term performance of heuristics or agent-based simulation models. Although Wang, Agatz, and Erera (2018) first mentioned the concept of stability for ride-sharing systems, their stability concept is the stable matching problem (Gusfield and Irving 1989). In contrast, the stability definition in our research is the boundedness of the queue lengths of waiting passengers. Furthermore, some experimental settings like fixed traveller agent waiting times lacked realism. Hörl, Becker, and Axhausen (2021) used MATsim to test the waiting time relationship with SAV sizes and found that different SAV sizes can result in

different passenger waiting times. Moreover, if passengers wait for a long time, some of them may leave the waiting queue to choose other alternative travel modes such as public transit and human-driven vehicles. Guo, Chen, and Liu (2022) aimed to optimise the SAV assignment and SAV relocation decisions based on a mixed-integer non-convex problem that integrates a discrete choice model to consider the alternative travel modes, human-driven vehicles. Reinforcement learning has been widely used in transportation studies recently (Liu et al. 2022; Ke et al. 2020; Yang et al. 2019). Liu et al. (2022) proposed a deep reinforcement learning approach for vehicle dispatching on the online ride-hailing platform with order cancellation data. Although they used real-world data, they studied the human-driven taxi market. Overall, no previous studies addressed the optimal SAV dispatching problem, stability of SAV systems, and modelling the passenger queueing dynamic with exiting passengers at the same time. This paper aims to provide an optimal SAV dispatch policy with a dynamic queuing model for waiting passengers that consider the possibility of exiting passengers and provide stability analysis when demand is within and outside of the stable region (Li et al. 2021; Kang and Levin 2021; Levin 2022).

2.2. Max-pressure control

Initially, max-pressure control was introduced as a scheduling strategy in communication and power systems (Tassiulas and Ephremides 1990). Varaiya (2013) converted it to a decentralised traffic signal control policy that guarantees network stability whenever possible. Max-pressure control defines the pressures of each turning movement then find the phase with the maximum pressure for each iteration. In addition, it is also a decentralised algorithm that can be computed separately for each individual intersection.

The excellent properties of max-pressure control have led many researchers to introduce it into the area of traffic signal control (Barman and Levin 2022, 2023; Xu et al. 2022; Xu, Bika, Levin n.d. b). Sun and Yin (2018) used the Vissim platform to study several recently proposed traffic signal control methods. The results showed that max-pressure control achieved better control performance of adaptive signal control systems. Also, the cycle-based max-pressure control seems to perform worse than the original non-cyclic max-pressure control.

Inspired by Varaiya (2013), we propose a linear programme to determine a stable SAVs dispatch policy without ride-sharing. Unlike the previous queuing models (Zhang, Rossi, and Pavone 2016), this model explicitly matches passengers to vehicles at different locations, meaning that we assign specific vehicles to specific passengers. Ideally, this dispatch strategy for SAVs services would maintain the stability of the largest set of demands possible. The only other studies on the stability of passenger waiting for queue lengths for SAVs, Li et al. (2021), Kang and Levin (2021), and Levin (2022), did not take exiting passengers into consideration due to the complexity of the stability proof. However, in reality, waiting for passengers will not wait indefinitely for SAVs and will instead switch to other travel modes, like public transit. Li et al. (2021) used a different state than the version presented here: they model the state as the waiting time of passengers. Since we want to characterise the stable region with specific mathematical equations that are related to demand and SAVs' fleet size, we use the passengers' waiting queue length as the state. The stable region is the set of passengers' travel demands that can be served by a given SAVs fleet size. Based on the characterised stable region with passengers' waiting queue length, we can analytically prove

the stability of our proposed dispatch policy and find the maximum stable demand. Kang and Levin (2021) used a similar queueing model and developed a max-stability dispatch policy based on the model predictive control. The output of their optimisation problem includes a sequence of controls for a planning horizon, which requires much more computation time. In this paper, we first prove the maximum stability property of a mixed integer linear programme for a queueing model without exiting passengers. Then, we extend the queueing model to exiting passengers, and show that the proposed fast maximum stability SAV dispatch policy still achieves maximum stability. Levin (2022) is the most recent paper that provided a maximum stability dispatch policy considering SAV behaviours such as charging, ridesharing, and integration with bus vehicles. Levin (2022) used the same state model as Li et al. (2021) However, they did not model the complex dynamic of exiting passengers into passenger queueing dynamics. To the best of our knowledge, this study is the first to provide maximum stability dispatching policy and models the dynamics of waiting for passengers and exiting passengers at the same time.

3. Basic stability analysis

3.1. Math notations

Table 1. Notation (without exiting passengers).

$\mathcal{N}$	Set of nodes
$\mathcal{A}$	Set of links
C_{qrs}	Travel time from node q to node r to s
$w_{rs}(t)$	Number of travellers at r waiting to be picked up to travel to s
$d_{rs}(t)$	The additional demand for travel from r to s at time t
$v_{qrs}(t)$	Number of SAVs assigned to travel from q to r to carry a passenger from r to s
$x_q^{\tau}(t)$	Number of vehicles that are τ time steps away from arriving at q
F	Fleet size of SAVs

3.2. Queueing model

In this section, we do not include exiting passengers; we will consider exiting passengers in Section 4. Consider a network $\mathcal{G} = (\mathcal{N}, \mathcal{A})$ with nodes $\mathcal{N}$ and links $\mathcal{A}$. Nodes represent locations where passengers are picked up and dropped off. We assume that SAVs have unlimited parking at nodes. We assume constant travel times. Links between nodes are not explicitly characterised, but are used to define the travel times. Let C_{qrs} be the travel time from node q to node r to node s. Note that, once a passenger is matched with a SAV, we assume that the passenger accepts the match. Let $w_{rs}(t)$ be the number of travellers at r waiting to be picked up to travel to s. Let $d_{rs}(t)$ be the additional demand for travel from r to s at time t. $d_{rs}(t)$ is a random variable with mean $\bar{d}_{rs}$ and maximum value $\hat{d}_{rs}$. Let $v_{qrs}(t)$ be the number of SAVs assigned to travel from q to r to carry a passenger from r to s. In defining $v_{qrs}(t)$, it is possible to have $q = r$. We assume that vehicles carry one passenger at a time. Then $w_{rs}(t)$ evolves as follows:

$$w_{rs}(t+1) = w_{rs}(t) + d_{rs}(t) - \sum_{q \in \mathcal{N}} v_{qrs}(t) \tag{1}$$

We require that $\sum_{q\in\mathcal{N}} v_{qrs}(t) \leq w_{rs}(t)$, i.e. vehicles cannot be dispatched to serve a passenger from r to s unless a traveller is waiting. Equation (1) does not model passengers exiting the system due to high waiting times. We will address such behaviour in Section 4 as it makes the stability analysis more complex.

We also track SAV locations. Let $x_q(t)$ be the number of SAVs parked at node q at time t. $x_q(t)$ bounds the number of vehicles that can be dispatched via

$$\sum_{(r,s)\in\mathcal{N}^2} v_{qrs}(t) \leq x_q(t) \quad \forall q \in \mathcal{N} \tag{2}$$

Once dispatched on a trip from q to r to s, vehicles will travel through the network for some time C_{qrs} before arriving at s. Therefore, we must also track SAVs that are enroute. Note that we assume the fleet size in the network is fixed, which means no SAV enters or exits the network. Although a fleet of human-driven ride-sharing vehicles will vary over time, a fleet of company-owned SAVs is not limited by driver working hours. Specifically, human drivers may reject the request from the central dispatcher due to some reasons such as fatigue or lower compensation. However, we assume that the operator can control all SAVs without limitation. Specifically, once a SAV finishes one trip, this SAV can be dispatched again on an empty trip to serve the next waiting passenger, the total number of serving vehicles in the system will not change (including vehicles in service and vehicles not in service). Let $x_q^\tau(t)$ be the number of vehicles that are τ time steps away from arriving at q. $x_q(t) = x_q^0(t)$. $x_q^\tau(t)$ evolves as follows:

$$x_q^\tau(t+1) = \begin{cases} x_q^{\tau+1}(t) + \sum\limits_{(s,r)\in\mathcal{N}^2: C_{srq}-1=\tau} v_{srq}(t) & \tau \geq 1 \\ x_q^0(t) + x_q^1(t) - \sum\limits_{(r,s)\in\mathcal{N}^2} v_{qrs}(t) & \tau = 0 \end{cases} \tag{3}$$

When a SAV departs on trip $[q, r, s]$ at time t, then the SAV will arrive at s at time $t + C_{qrs}$. Then at time $t + 1$ it will have $C_{qrs} - 1$ travel time remaining, so that SAV is added to $x_s^{C_{qrs}-1}(t+1)$.

$x_q^\tau(t)$ defines the locations of all SAVs in the network. Therefore, the fleet size F can be related to SAV locations via

$$F = \sum_{q\in\mathcal{N}} \sum_{\tau=0}^{\infty} x_q^\tau(t) \tag{4}$$

The state consists of the waiting passenger queues and SAV locations, i.e. $\mathbf{w}(t)$ and $\mathbf{x}(t)$. The control is $v_{qrs}(t)$, and the control space varies based on the available SAVs defined by $\mathbf{x}(t)$.

3.3. Stable network

We define the *stability* of the network as follows:

Definition 3.1: The network is stable if the number of waiting passengers remains bound on average, i.e. there exists a $\kappa < \infty$ such that

$$\lim_{T\to\infty} \frac{1}{T} \sum_{t=1}^{T} \sum_{(r,s)\in\mathcal{N}^2} w_{rs}(t) \leq \kappa \tag{5}$$

Equation (5) means that the number of passengers remains bounded over time. We also want to emphasise the practical meaning of stable and unstable networks. In practice, the network is stable if the passenger demand rate is the same as the SAV service rate, so SAVs will serve all passengers with finite waiting times. Ensuring a stable network is hard in reality, but it is an important modelling concept since it requires that passengers can be served as soon as possible. Since passengers can only exit the network by travelling via SAV, stability requires that sufficient SAV service throughput is provided to ensure passenger queues will not grow to infinity. Contrary to a stable network, an unstable network means that the number of waiting passengers is not bound over time. Intuitively, an unstable network means that the rate of passengers' requests is larger than the SAV service rate. Thus some passengers will not be served.

3.4. FMS-dispatch: fast maximum stability dispatch policy

The proposed policy $\pi^\star$ is defined as follows. At each time step t, solve the integer linear program

$$\min \quad \sum_{(q,r,s)\in\mathcal{N}^3} v_{qrs}(t)C_{qrs} \tag{6a}$$

$$\text{s.t.} \quad \sum_{q\in\mathcal{N}} v_{qrs}(t) \le w_{rs}(t) \qquad \forall (r,s)\in\mathcal{N}^2 \tag{6b}$$

$$\sum_{(r,s)\in\mathcal{N}^2} v_{qrs}(t) \le x_q(t) \qquad \forall q\in\mathcal{N} \tag{6c}$$

$$\sum_{(q,r,s)\in\mathcal{N}^3} v_{qrs}(t) = \min\left\{\sum_{(r,s)\in\mathcal{N}^2} w_{rs}(t), \sum_{q\in\mathcal{N}} x_q(t)\right\} \tag{6d}$$

$$v_{qrs}(t)\in\mathbb{Z}_+ \qquad \forall (q,r,s)\in\mathcal{N}^3 \tag{6e}$$

Equation (6a) means that this dispatch policy is based on minimising the total SAVs travel time at each time step. Idle SAVs can accept passengers' requests right away, but vehicles in service cannot accept passengers' requests until they finish their trips. The dispatcher wants to achieve its objective at the time of SAVs assignment without requiring a planning time horizon. Furthermore, this dispatcher only focuses on real-time demand and does not consider the empty vehicle relocation based on the near-future demand. We are working on integrating empty vehicle relocation into the maximum stability dispatch policy in another paper. Equation (6b) indicates that SAVs can only be dispatched unless there are passengers waiting. Consequently, our model does not account for a preemptive rebalancing of SAVs. However, if Equation (6b) is violated, then it is possible that SAVs are assigned to preemptive rebalancing. Consequently, the systems will not reach maximum stability since the SAVs assigned to preemptive relocation are not serving passengers, which could reduce the rate of passengers served. Furthermore, Equation (6d) is necessary to avoid the trivial solution $v_{qrs}(t) = 0$ by requiring that the number of vehicles dispatched is either equal to the number of waiting passengers or the number of available vehicles, whichever is smaller. In problem (6a), $w_{rs}(t)$ and $x_q(t)$ are exogenous. $x_q^\tau(t)$ is the current state of systems, i.e. the

current location of SAVs. We cannot change the current state; we can only control decisions affecting the future state. The decision variables are $v_{qrs}(t)$. The resulting optimal solution $v^{\star}_{qrs}(t)$ is used to determine which SAVs to dispatch and which passengers they are assigned to serve. We will prove the stability properties of $\pi^{\star}$ in Section 3.6. If $v_{qrs}(t) = 0$, there is no SAV to serve passengers, which results in the average number of waiting for passengers growing to infinity. In other words, the network would be always unstable since some waiting passengers would not be served. Note that C_{qrs} is deterministic, and we can not handle time-dependent travel time due to the complexity of stability analysis in this paper. We hope to conduct time-dependent travel time analysis in the future with traffic flow models such as the cell transmission model to consider congestion-aware travel time for future study. However, we can handle independent and identical distributed random travel times in this model. For instance, we could generate travel times for different trips from q to r to s based on some distributions (such as poisson distribution), the evolutions of Equations (3) and (4) are related to the newly independent and identical travel times. The stable region will not change either since it it related to average travel time, which can be obtained based on the distribution of travel times. Furthermore, the maximum-stability dispatching policy will not change either, the corresponding travel time C_{qrs} will become a random and identical variable based on some distributions.

3.5. Stable region

For any given fleet size, it is easily possible to find an average demand rate that cannot be stabilised. If the demand is sufficiently high, no SAV dispatch policy will be able to serve all passengers. Therefore, it is necessary to characterise the stable region of demand given a fleet size. Stable region is the set of demands that could be served by a given fleet size under any dispatch policy. We then show that the max-pressure policy will stabilise any demand within the stable region. Consider a dispatch policy defining a sequence of vehicle trips $v_{qrs}(t)$. Let $\bar{v}_{qrs}$ be the average number of vehicles dispatched from q to r to s per time step, defined as

$$\bar{v}_{qrs} = \lim_{T\to\infty} \frac{1}{T} \sum_{t=1}^{T} v_{qrs}(t) \tag{7}$$

This $\bar{v}_{qrs}$ can be related to passenger demand to determine which average demand rates $\bar{\mathbf{d}}$ can be served by a given fleet size F. These constraints hold on average, but stochastic variations in demand necessitate a corresponding response. Even with deterministic demand, it may not be possible to dispatch SAVs according to the values of $\bar{v}_{qrs}$ because $\bar{v}_{qrs} \in \mathbb{R}_+$ whereas $v_{qrs}(t) \in \mathbb{Z}_+$.

First, it is necessary to serve all demands, resulting in the constraint

$$\sum_{q\in\mathcal{N}} \bar{v}_{qrs} = \bar{d}_{rs} \quad \forall (r,s) \in \mathcal{N}^2 \tag{8}$$

Constraint (8) is given with strict equality because SAVs are assumed to only make trips when a passenger is waiting. SAVs must obey conservation of flow, so the number of SAVs

incoming to s must equal the number of SAVs outgoing from s:

$$\sum_{(q,r)\in\mathcal{N}^2} \bar{v}_{qrs} = \sum_{(q,r)\in\mathcal{N}^2} \bar{v}_{sqr} \quad \forall s \in \mathcal{N} \tag{9}$$

The number of SAVs that can be dispatched at any time step is bounded by F. Once dispatched on a trip from q to r to s, which dispatch affects C_{qrs} time steps. Consequently, over a long time horizon T,

$$\sum_{t=1}^{T} \sum_{(q,r,s)\in\mathcal{N}^3} v_{qrs}(t) C_{qrs} \leq F \times T \tag{10}$$

Here is an example for better understanding Equation (10). Suppose that we have only one SAV (fleet size $F = 1$) in the entire network with simulation time horizon $T = 10$ time steps, and this SAV is dispatched travel from q to serve a passenger goes from r to s. The travel time for SAV is $C_{qrs} = 6$ time steps. At this point, no SAVs in the network can be dispatched until this vehicle finishes this trip, which costs C_{qrs} time steps. Therefore, Equation (10) gives us the constraints $1 \times 6 \leq 1 \times 10$.

Moving on, we take the limit as $T \to \infty$ for Equation (10) yields

$$\lim_{T\to\infty} \frac{1}{T} \sum_{t=1}^{T} \sum_{(q,r,s)\in\mathcal{N}^3} v_{qrs}(t) C_{qrs} \leq F \tag{11}$$

or equivalently

$$\sum_{(q,r,s)\in\mathcal{N}^3} \bar{v}_{qrs} C_{qrs} \leq F \tag{12}$$

Based on Equation (12), we can define an average time $\bar{C}_{rs}$ required to serve a passenger from r to s. This time includes C_{rs} and the empty travel time required to send a vehicle to r:

$$\bar{C}_{rs} = \frac{\sum_{q\in\mathcal{N}} \bar{v}_{qrs} C_{qrs}}{\sum_{q\in\mathcal{N}} \bar{v}_{qrs}} \tag{13}$$

Using Equations (12) and (13) can be rewritten as

$$\sum_{(r,s)\in\mathcal{N}^2} \bar{C}_{rs} \sum_{q\in\mathcal{N}} \bar{v}_{qrs} \leq F \tag{14}$$

Combining Equations (7) and (14) yields

$$\sum_{(r,s)\in\mathcal{N}^2} \bar{C}_{rs} \bar{d}_{rs} \leq F \tag{15}$$

Let $\mathcal{D}$ be the set of demands for which there exists a $\bar{\mathbf{v}}$ satisfying constraints (8), (9) and (12). Let $\mathcal{D}^0$ be the interior of $\mathcal{D}$, i.e. where constraint (12) holds with strict inequality. Then there exists an $\epsilon > 0$ such that

$$\sum_{(r,s)\in\mathcal{N}^2} \bar{C}_{rs} \bar{d}_{rs} - F = \sum_{(q,r,s)\in\mathcal{N}^3} \bar{v}_{qrs} C_{qrs} - F \leq -\epsilon \tag{16}$$

Proposition 3.1: *If $\bar{\mathbf{d}} \notin \mathcal{D}$, then there does not exist a stabilising control.*

$\mathcal{D}$ is the set of demands that can be served by any dispatch policy, including others that have previously been published in the literature (Kang and Levin 2021; Li et al. 2021; Levin 2022). However, $\bar{d}$ does not belong to $\mathcal{D}$ means the demand for passengers is too large and no dispatch policy can serve this set of demands.

Proof: If the network is unstable, the passengers' demand is greater than the SAVs' supply. Since $\bar{\mathbf{d}} \notin \mathcal{D}, \forall \sum_{q\in\mathcal{N}} \bar{v}_{qrs}(t)$, there exists $\theta > 0$ and origin-destination pair (r, s) satisfy $\bar{d}_{rs} \geq \sum_{q\in\mathcal{N}} \bar{v}_{qrs} + \theta$.

Based on Equation (1) we further obtain:

$$w_{rs}(t+1) - w_{rs}(t) = d_{rs}(t) - \sum_{q\in\mathcal{N}} v_{qrs}(t) \tag{17}$$

Based on Equation (17) we can derive the following relationship:

$$\mathbb{E}\left[\sum_{t=0}^{\tau-1}\sum_{(r,s)\in\mathcal{N}^2}(w_{rs}(t+1) - w_{rs}(t))\right] = \mathbb{E}\left[\sum_{(r,s)\in\mathcal{N}^2} w_{rs}(\tau) - w_{rs}(0)\right] \tag{18}$$

$$= \mathbb{E}\left[\sum_{(r,s)\in\mathcal{N}^2}(\bar{d}_{rs} - \sum_{q\in\mathcal{N}}\bar{v}_{qrs})\right] \tag{19}$$

$$\geq \mathbb{E}\left[\tau\theta\right] = \tau\theta \tag{20}$$

Move $w_{rs}(0)$ to the right hand side, we obtain:

$$\mathbb{E}\left[\sum_{(r,s)\in\mathcal{N}^2}(w_{rs}(\tau))\right] \geq \theta\tau + \mathbb{E}\left[\sum_{(r,s)\in\mathcal{N}^2}(w_{rs}(0))\right] \tag{21}$$

or equivalently

$$\mathbb{E}\left[|\mathbf{w}(\tau)|\right] \geq \theta\tau + \mathbb{E}\left[|\mathbf{w}(0)|\right] \tag{22}$$

From Equation (22), we get

$$\lim_{T\to\infty}\mathbb{E}\left[\frac{1}{T}\sum_{t=1}^{T}|\mathbf{w}(t)|\right] \geq \lim_{T\to\infty}\frac{1}{T}\sum_{t=1}^{T}\mathbb{E}\left[\theta t + \mathbb{E}\left[|\mathbf{w}(0)|\right]\right] = \infty \tag{23}$$

Based on (22), $w_{rs}(t)$ will increase by θ in each step. Therefore, we can conclude based on Equation (23), $w_{rs}(t)$ will increase to infinity, which violates Equation (5). ■

3.6. Stability analysis

We now proceed to prove that the policy $\pi^\star$ defined in Section 3.4 will stabilise any demand $\bar{\mathbf{d}} \in \mathcal{D}^0$. Since any demand $\bar{\mathbf{d}} \notin \mathcal{D}$ cannot be stabilised by Proposition 3.1, this essentially proves that $\pi^\star$ achieves maximum stability. The only excluded demand is on the boundary of $\mathcal{D}$, for which the Markov chain can be shown to be null recurrent but not positive recurrent.

Lemma 3.1: *When policy $\pi^\star$ is used and $\bar{\mathbf{d}} \in \mathcal{D}^0$, there exists a Lyapunov function $v(t) \geq 0$ and constants $\kappa > 0, \epsilon > 0$ such that*

$$\mathbb{E}\left[v(t+1) - v(t) | \, \mathbf{w}(t), \mathbf{x}(t) \right] \leq \kappa - \epsilon |\mathbf{w}(t)| \tag{24}$$

Proof: Consider the Lyapunov function

$$v(t) = \left(\sum_{(r,s)\in\mathcal{N}^2} w_{rs}(t) \right) \left(\sum_{(r,s)\in\mathcal{N}^2} \frac{\bar{C}_{rs} w_{rs}(t)}{2} \right) + \left(\sum_{(r,s)\in\mathcal{N}^2} w_{rs}(t) \right) \left(\sum_{s\in\mathcal{N}} \sum_{\tau=1}^{\infty} \tau x_s^\tau(t) \right) \tag{25}$$

For ease of presentation, define $v(t) = v_1(t) + v_2(t)$ where

$$v_1(t) = \left(\sum_{(r,s)\in\mathcal{N}^2} w_{rs}(t) \right) \left(\sum_{(r,s)\in\mathcal{N}^2} \frac{\bar{C}_{rs} w_{rs}(t)}{2} \right) \tag{26}$$

and

$$v_2(t) = \left(\sum_{(r,s)\in\mathcal{N}^2} w_{rs}(t) \right) \left(\sum_{s\in\mathcal{N}} \sum_{\tau=1}^{\infty} \tau x_s^\tau(t) \right) \tag{27}$$

First, we expand the difference $v_1(t+1) - v_1(t)$. Let $\delta_{rs}(t) = w_{rs}(t+1) - w_{rs}(t)$. Then

$$\begin{aligned} v_1(t+1) - v_1(t) &= \left(\sum_{(r,s)\in\mathcal{N}^2} w_{rs}(t+1) \right) \left(\sum_{(r,s)\in\mathcal{N}^2} \frac{\bar{C}_{rs} w_{rs}(t+1)}{2} \right) \\ &\quad - \left(\sum_{(r,s)\in\mathcal{N}^2} w_{rs}(t) \right) \left(\sum_{(r,s)\in\mathcal{N}^2} \frac{\bar{C}_{rs} w_{rs}(t)}{2} \right) \qquad (28) \\ &= \left(\sum_{(r,s)\in\mathcal{N}^2} w_{rs}(t) + \delta_{rs}(t) \right) \left(\sum_{(r,s)\in\mathcal{N}^2} \frac{\bar{C}_{rs}}{2} \left(w_{rs}(t) + \delta_{rs}(t) \right) \right) \\ &\quad - \left(\sum_{(r,s)\in\mathcal{N}^2} w_{rs}(t) \right) \left(\sum_{(r,s)\in\mathcal{N}^2} \frac{\bar{C}_{rs} w_{rs}(t)}{2} \right) \qquad (29) \\ &= \left(\sum_{(r,s)\in\mathcal{N}^2} \delta_{rs}(t) \right) \left(\sum_{(r,s)\in\mathcal{N}^2} \frac{\bar{C}_{rs} \delta_{rs}(t)}{2} \right) \\ &\quad + \left(\sum_{(r,s)\in\mathcal{N}^2} \bar{C}_{rs} \delta(t) \right) \left(\sum_{(r,s)\in\mathcal{N}^2} w_{rs}(t) \right) \qquad (30) \end{aligned}$$

We will show that $(\sum_{(r,s)\in\mathcal{N}^2} \delta_{rs}(t))(\sum_{(r,s)\in\mathcal{N}^2} \frac{\bar{C}_{rs}\delta_{rs}(t)}{2})$ is bounded and leave the second term for later.

$$\left(\sum_{(r,s)\in\mathcal{N}^2} \delta_{rs}(t) \right) \left(\sum_{(r,s)\in\mathcal{N}^2} \frac{\bar{C}_{rs} \delta_{rs}(t)}{2} \right) \leq \left(\sum_{(r,s)\in\mathcal{N}^2} \hat{d}_{rs} \right) \left(\sum_{(r,s)\in\mathcal{N}^2} \frac{\bar{C}_{rs} \hat{d}_{rs}(t)}{2} \right) \tag{31}$$

since $w_{rs}(t+1) - w_{rs}(t)$ increases by at most $\hat{d}_{rs}$, the maximum value of $d_{rs}(t)$.

Now we continue working with $\nu_2(t+1) - \nu_2(t)$.

$$\nu_2(t+1) - \nu_2(t)$$

$$= \left(\sum_{(r,s)\in\mathcal{N}^2} w_{rs}(t+1) \right) \left(\sum_{s\in\mathcal{N}} \sum_{\tau=1}^{\infty} x_s^\tau(t+1) \right) - \left(\sum_{(r,s)\in\mathcal{N}^2} w_{rs}(t) \right) \left(\sum_{s\in\mathcal{N}} \sum_{\tau=1}^{\infty} \tau x_s^\tau(t) \right) \tag{32}$$

$$= \delta(t) \left(\sum_{s\in\mathcal{N}} \sum_{\tau=1}^{\infty} \tau x_s^\tau(t+1) \right) - \left(\sum_{(r,s)\in\mathcal{N}^2} w_{rs}(t) \right) \left(\sum_{s\in\mathcal{N}} \sum_{\tau=1}^{\infty} \tau \left(x_s^\tau(t+1) - x_s^\tau(t) \right) \right) \tag{33}$$

The first term is bound because $\sum_{\tau=1}^{\infty} x_s^\tau(t+1) \le F$, so

$$\delta(t) \left(\sum_{s\in\mathcal{N}} \sum_{\tau=1}^{\infty} \tau x_s^\tau(t+1) \right) \le \left(\sum_{(r,s)\in\mathcal{N}^2} \hat{d}_{rs} \right) \left(F \times \max_{(q,r,s)\in\mathcal{N}^3} \{C_{qrs}\} \right) \tag{34}$$

We are now left with the difference $(\sum_{(r,s)\in\mathcal{N}^2} w_{rs}(t))(\sum_{(r,s)\in\mathcal{N}^2} \bar{C}_{rs}\delta_{rs}(t) + \sum_{s\in\mathcal{N}} \sum_{\tau=1}^{\infty} \tau (x_s^\tau(t+1) - x_s^\tau(t)))$. First, observe that from Equation (3),

$$\sum_{\tau=1}^{\infty} \tau x_s^\tau(t+1) - \sum_{\tau=1}^{\infty} \tau x_s^\tau(t) = \sum_{\tau=1}^{\infty} (\tau-1) x_s^{\tau-1}(t+1) - \sum_{\tau=1}^{\infty} \tau x_s^\tau(t) \tag{35}$$

$$= \sum_{\tau=1}^{\infty} (\tau-1) x_s^\tau(t) - \sum_{\tau=1}^{\infty} \tau x_s^\tau(t) + \sum_{(q,r,s)\in\mathcal{N}^3} v_{qrs}(t) C_{qrs} \tag{36}$$

$$= -\sum_{\tau=0}^{\infty} x_s^\tau(t) + \sum_{(q,r,s)\in\mathcal{N}^3} v_{qrs}(t) C_{qrs} \tag{37}$$

$$= -F + \sum_{(q,r,s)\in\mathcal{N}^3} v_{qrs}(t) C_{qrs} \tag{38}$$

From Equation (17),

$$\bar{C}_{rs}\delta_{rs}(t) = \bar{C}_{rs} \left(d_{rs}(t) - \sum_{q\in\mathcal{N}} v_{qrs}(t) \right) \tag{39}$$

Combining Equations (33) and (39) yields

$$\mathbb{E}\left[\left(\sum_{(r,s)\in\mathcal{N}^2} w_{rs}(t) \right) \left(\sum_{(r,s)\in\mathcal{N}^2} \bar{C}_{rs}\delta_{rs}(t) + \sum_{s\in\mathcal{N}} \sum_{\tau=1}^{\infty} \tau \left(x_s^\tau(t+1) - x_s^\tau(t) \right) \right) \middle| \mathbf{w}(t), \mathbf{x}(t) \right]$$

$$= \mathbb{E}\left[\left(\sum_{(r,s)\in\mathcal{N}^2} w_{rs}(t) \right) \left(\left(\sum_{(r,s)\in\mathcal{N}^2} \bar{C}_{rs} \left(d_{rs}(t) - \sum_{q\in\mathcal{N}} v_{qrs}(t) \right) \right) - F \right.\right.$$

$$\left.\left. + \sum_{(q,r,s)\in\mathcal{N}^3} v_{qrs}(t) C_{qrs} \right) \middle| \mathbf{w}(t), \mathbf{x}(t) \right] \tag{40}$$

Notice that

$$\mathbb{E}\left[\left(\sum_{(r,s)\in\mathcal{N}^2} w_{rs}(t)\right)\left(-F+\sum_{(r,s)\in\mathcal{N}^2}\bar{C}_{rs}d_{rs}(t)\right)\middle|\mathbf{w}(t),\mathbf{x}(t)\right]$$

$$=\left(\sum_{(r,s)\in\mathcal{N}^2} w_{rs}(t)\right)\left(-F+\sum_{(r,s)\in\mathcal{N}^2}\bar{C}_{rs}\bar{d}_{rs}\right) \tag{41}$$

$$=-\epsilon|\mathbf{w}(t)| \tag{42}$$

since $F\geq\sum_{(r,s)\in\mathcal{N}^2}\bar{C}_{rs}\bar{d}_{rs}$ by Equation (12). Let $v^{\star}_{qrs}(t)$ be chosen by $\pi^{\star}$. Recall that there exists a $v_{qrs}(t)$ defining the stable region such that the average travel time required to serve origin-destination pair (r,s) is $\bar{C}_{rs}$. Then we have

$$\mathbb{E}\left[\left(\sum_{(r,s)\in\mathcal{N}^2} w_{rs}(t)\right)\left(\sum_{(q,r,s)\in\mathcal{N}^3} v^{\star}_{qrs}(t)C_{qrs}\right)\middle|\mathbf{w}(t),\mathbf{x}(t)\right]$$

$$\leq\mathbb{E}\left[\left(\sum_{(r,s)\in\mathcal{N}^2} w_{rs}(t)\right)\left(\sum_{(q,r,s)\in\mathcal{N}^3} v_{qrs}(t)C_{qrs}\right)\middle|\mathbf{w}(t),\mathbf{x}(t)\right]$$

$$=\sum_{(q,r,s)\in\mathcal{N}^3} v_{qrs}(t)\bar{C}_{rs} \tag{43}$$

Equation (24) follows from Equations (42) and (43). ■

Proposition 3.2: *When policy $\pi^{\star}$ is used and $\bar{\mathbf{d}}\in\mathcal{D}^0$, the network is stable.*

Proof: Follows from Lemma 3.1. For inequality (24), taking expectations and summing over $t=1,\ldots,T$ yields the following inequality:

$$\mathbb{E}\left[\nu(T+1)-\nu(1)|\,\mathbf{w}(t),\mathbf{x}(t)\right]\leq\kappa T-\epsilon\sum_{t=1}^{T}|\mathbf{w}(t)| \tag{44}$$

and so,

$$\epsilon\frac{1}{T}\sum_{t=1}^{T}\mathbb{E}\left[|\mathbf{w}(t)|\right]\leq\kappa-\frac{1}{T}\mathbb{E}\left[\nu(T+1)\right]+\frac{1}{T}\mathbb{E}\left[\nu(1)\right]\leq\kappa+\frac{1}{T}\mathbb{E}\left[\nu(1)\right] \tag{45}$$

which immediately implies that the stability Definition 3.1 is satisfied. ■

Proposition 3.3: *The maximum stable demand $\sum_{(r,s)\in\mathcal{N}^2}\bar{d}_{rs}$ increases linearly with the fleet size F*

Proof: Consider a certain fleet size F. Combining constraints (8), (9) and (12), we obtain:

$$\alpha\sum_{(r,s)\in\mathcal{N}^2}\bar{d}_{rs}\bar{C}_{rs}=\alpha\sum_{(q,r,s)\in\mathcal{N}^3}\bar{v}_{qrs}C_{qrs}\leq\alpha F \tag{46}$$

Multiplying F by the factor α results in a same proportion change in $\sum_{(r,s)\in\mathcal{N}^2}\bar{d}_{rs}$. ■

4. Extension to exiting passengers

4.1. Math notation considering exiting passengers

Table 2. Notation (exiting passengers).

$\mathcal{N}$	Set of nodes
$\mathcal{A}$	Set of links
$w_{rs}^{\phi}(t)$	Number of travellers at r waiting to be picked up to travel to s who have been waiting for ϕ time step at time step t
$e_{rs}^{\phi}(t)$	Number of travellers that exit due to waiting times who have been waiting for ϕ time steps at time step t
$v_{qrs}^{\phi}(t)$	Number of SAVs assigned to travel from q to r to carry passengers who have been waiting for ϕ time step to be picked up from r to s
$x_q^{\tau}(t)$	Number of vehicles that are τ time steps away from arriving at q
Φ	Maximum waiting time of passengers in a city network

In Section 3, travellers were modelled as waiting at their origin until they are served. In reality, travellers are likely to exit the system if waiting times become too high. Notice that the number of exiting passengers depends on the waiting time. The longer the waiting times, the higher the rate at which passengers leave the queue. Therefore, we define the number of travellers at r waiting to be picked up to travel to s at time steps t who have been waiting for ϕ time step as $w_{rs}^{\phi}(t)$. For instance, the number of travellers at r waiting to be picked up to travel to s at time step 3 who has waiting for 2-time steps can be denoted as $w_{rs}^{2}(3)$. Let $e_{rs}^{\phi}(t)$ be the number of travellers that exit due to waiting times who have been waiting for ϕ time steps. Let $v_{qrs}^{\phi}(t)$ be the number of SAVs assigned to travel from q to r to carry passengers who have been waiting for ϕ time step to be picked up from r to s. Then Equation (1) is modified to include waiting times ϕ and exiting passengers $e_{rs}^{\phi}(t)$ as follows:

$$w_{rs}^{\phi+1}(t+1) = \begin{cases} w_{rs}^{\phi}(t) - e_{rs}^{\phi}(t) - \sum_{q\in\mathcal{N}} v_{qrs}^{\phi}(t) & \phi \geq 1 \\ d_{rs}(t) - \sum_{q\in\mathcal{N}} v_{qrs}^{\phi}(t) & \phi = 0 \end{cases} \tag{47}$$

We assume that $e_{rs}^{0}(t) = 0$, and $\max\{\phi\} = \Phi$, where Φ is defined as the maximum waiting time of passengers in a city network. It is reasonable to have $\Phi \leq \infty$ because passengers will not wait infinitely long for pick-up. Furthermore, $e_{rs}^{\phi}(t)$ is a random variable that is related to waiting time ϕ, and $\sum_{q\in\mathcal{N}} v_{qrs}^{\phi}(t)$ will first pick up travellers who have waiting for a longer time ϕ. Also, $v_{qrs}^{1}(t) > 0$ only if $v_{qrs}^{2}(t) = w_{rs}^{2}(t)$. $\sum_{q\in\mathcal{N}} \sum_{\phi=0}^{\Phi} v_{qrs}^{\phi}(t)$ is the total number of dispatched vehicles for (r, s), i.e. $\sum_{q\in\mathcal{N}} \sum_{\phi=0}^{\Phi} v_{qrs}^{\phi}(t) = \sum_{q\in\mathcal{N}} v_{qrs}(t)$.

We use a small example to explain the evolution of waiting for passengers including exiting passengers: Assuming $w_{rs}^{1}(t) = 10$, $w_{rs}^{2}(t) = 8$, since the higher waiting time ϕ, the smaller the number of waiting passengers. Suppose that $e_{rs}^{1}(t) = 2$ and $e_{rs}^{2}(t) = 4$. Therefore, the evolution is shown as follows:

$$w_{rs}^{2}(t+1) = w_{rs}^{1}(t) - e_{rs}^{1}(t) - \sum_{q\in\mathcal{N}} v_{qrs}^{1}(t) = 10 - 2 - 1 = 7 \tag{48}$$

$$w_{rs}^{3}(t+1) = w_{rs}^{2}(t) - e_{rs}^{2}(t) - \sum_{q\in\mathcal{N}} v_{qrs}^{2}(t) = 8 - 4 - 4 = 0 \tag{49}$$

4.2. Stable network

Stability must now be redefined because passengers will exit the system regardless of whether SAV service is provided. Therefore, queue lengths may remain bounded even if SAV service is insufficient. On average, $|\bar{\mathbf{d}}|$ new demand arrives each time step. Therefore, the average number of passengers exiting the system per time step because they are not served will also be bound by definition. Instead, we can define the cumulative number of unserved passengers $\omega(t)$ as

$$\omega(t) = \sum_{t'=1}^{t} \sum_{(r,s)\in\mathcal{N}^2} \sum_{\phi=0}^{\Phi} e_{rs}^{\phi}(t') \tag{50}$$

Equivalently, we can write a Markov equation for the cumulative number of unserved passengers:

$$\omega(t+1) = \omega(t) + \sum_{(r,s)\in\mathcal{N}^2} \sum_{\phi=0}^{\Phi} e_{rs}^{\phi}(t) \tag{51}$$

Ideally, the SAV system will serve almost all passengers. Network stability that relies on some origin-destinations being underserved does not achieve maximum throughput. In Section 3, it was required that all passengers were served for stability. However, due to stochasticity, it is possible that an unusually large number of passengers arrive at one time step. That will result in a correspondingly higher value of $e_{rs}^{\phi}(t)$, but should be balanced out with less demand and $e_{rs}^{\phi}(t) = 0$ at later time steps. If we take an average value of $\omega(t)$ over time, it should be zero if the network is stable.

Definition 4.1: The network is stable if the average cumulative number of unserved passengers in the long run equals zero.

$$\lim_{T\to\infty} \mathbb{E}\left[\frac{1}{T}\omega(T)\right] = 0 \tag{52}$$

Readers may notice that we use different indicators between Definitions 3.1 and 4.1 to represent the stable network. The reason we use different indicators is when we do not include exiting passengers, the evolution of the average number of waiting for passengers can reflect the stable and unstable network. However, the average number of waiting passengers is not a good indicator to a evaluate stable and unstable network when considering exiting passengers. The average number of waiting passengers can always be bounded when we allow passengers to exit the waiting queue at each time step if they do not want to wait (given a certain tolerance time). However, Definitions 3.1 and 4.1 have strong connections since they are both used to define whether all passengers are being served. We used the same dispatch policy for exiting and no exiting passengers scenarios. The only difference between the two scenarios is the queueing model. Please refer to Equations (1) and (48) for comparison.

4.3. Stable region with exiting passengers

Consider a dispatch policy defining a sequence of vehicle trips $v_{qrs}(t)$. The average number of vehicles dispatched from q to r to s is defined like Equation (7). As some passengers are

exiting the queuing system per time step, and the dispatched vehicle will pick up passengers who have been waiting for a longer time. Therefore, the dispatched vehicle at t time step has the following relationship with $v^{\phi}_{qrs}(t)$.

$$\sum_{q\in\mathcal{N}}\sum_{\phi=0}^{\Phi} v^{\phi}_{qrs}(t) = \sum_{q\in\mathcal{N}} v_{qrs}(t) \tag{53}$$

This $\bar{v}_{qrs}$ can be related to passenger demand with average exiting passengers $\bar{e}_{rs}$ to determine which average demand rates $\bar{\mathbf{d}}$ can be served by a given fleet size F. These constraints hold on average, but stochastic variations in demand necessitate a corresponding response. Even with a deterministic demand, it may not be possible to dispatch SAVs according to the values of $\bar{v}_{qrs}$ because $\bar{v}_{qrs} \in \mathbb{R}_+$ whereas $v_{qrs}(t) \in \mathbb{Z}_+$.

First, it is necessary to serve all demands except average exiting passengers $\bar{e}_{rs}$, resulting in the below constraint.

$$\sum_{q\in\mathcal{N}} \bar{v}_{qrs} = \bar{d}_{rs} - \bar{e}_{rs} \quad \forall (r,s) \in \mathcal{N}^2 \tag{54}$$

Constraint (54) is given with strict equality because SAVs are assumed to only make trips when a passenger is waiting. SAVs must obey the conservation of flow, which means that Equation (9) holds here too. The number of SAVs that can be dispatched at any time step is bound by the fleet size F. Once dispatched on a trip from q to r to s, that dispatch affects C_{qrs} time steps. Consequently, over a long time horizon T, we can get the same inequality as Equations (10)–(12).

We already defined an average time $\bar{C}_{rs}$ in Equations (13)–(14), which is required to serve a passenger from r to s. This time includes C_{rs} and also the empty travel required to send a vehicle to r.

Combining Equations (7) and (12) yields

$$\sum_{(r,s)\in\mathcal{N}^2} \bar{C}_{rs}(\bar{d}_{rs} - \bar{e}_{rs}) \leq F \tag{55}$$

$\mathcal{D}$ is defined as the set of demands already, for which there exists a $\bar{\mathbf{v}}$ satisfying constraints (8), (9) and (12). $\mathcal{D}^0$ is the interior of $\mathcal{D}$, which is also defined already, i.e. where constraint (11) holds with strict inequality. Then there exists an $\epsilon > 0$ such that

$$\sum_{(r,s)\in\mathcal{N}^2} \bar{C}_{rs}(\bar{d}_{rs} - \bar{e}_{rs}) - F = \sum_{(q,r,s)\in\mathcal{N}^3} \bar{v}_{qrs}C_{qrs} - F \leq -\epsilon \tag{56}$$

4.4. Stability analysis with exiting passengers

We now need to prove that the policy $\pi^\star$ defined in Section 3.4 will stabilise demand $\bar{\mathbf{d}} \in \mathcal{D}^0$ when some exiting passengers $\bar{\mathbf{e}}(t)$ are leaving the queuing system in each time step. The evolution of waiting for passengers can be described by the discrete-time Markov Chain with the state vector $\mathbf{w}(t)$ and $\mathbf{x}(t)$, and using Equation (47) for the evolution of $\mathbf{w}(t)$. We first prove Lemmas 4.1 and 4.2 to assist with the proof of stability.

Lemma 4.1: $\mathbb{E}\left[\sum_{\phi=1}^{\Phi} w_{rs}^{\phi}(t)\right]$ *is bounded by the positive constant* $\Phi\hat{d}_{rs}$.

$$\mathbb{E}\left[\sum_{\phi=1}^{\Phi} w_{rs}^{\phi}(t)\right] \leq \Phi\hat{d}_{rs} \tag{57}$$

The practical meaning of $\Phi\hat{d}_{rs}$ is the sum of total maximum demand from time step 1 to time step ϕ.

Proof: Since the number of waiting passengers at time step t should be less than or equal to the maximum demand $\hat{d}_r$ at each time step, we have:

$$w_{rs}^{\phi}(t) \leq \hat{d}_{rs} \quad \phi \geq 1 \tag{58}$$

We sum from 1 to Φ for each $w_{rs}^{\phi}(t)$ at time step t:

$$\mathbb{E}\left[\underbrace{w_{rs}^{1}(t) + w_{rs}^{2}(t) + \cdots + w_{rs}^{\Phi}(t)}_{\Phi}\right] \leq \Phi\hat{d}_{rs} \tag{59}$$

Then we have the following inequality

$$\mathbb{E}\left[\sum_{\phi=1}^{\Phi} w_{rs}^{\phi}(t)\right] \leq \Phi\hat{d}_{rs} \tag{60}$$

■

Lemma 4.2:

$$\mathbb{E}\left[\omega(t+1) - \omega(t)\right] \leq \sum_{(r,s)\in\mathcal{N}^2}\left(\Phi\hat{d}_{rs}\right) \tag{61}$$

Proof: The Markovian equation of the accumulative number of unserved passengers $\omega(t)$ is represented by Equation (51). After combining with and $\sum_{\phi=0}^{\Phi} e_{rs}^{\phi}(t) = 0$, we have

$$\mathbb{E}\left[\omega(t+1) - \omega(t)|\mathbf{e}(t)\right] = \mathbb{E}\left[\sum_{(r,s)\in\mathcal{N}^2}\sum_{\phi=0}^{\Phi} e_{rs}^{\phi}(t)\middle|\mathbf{e}(t)\right] \tag{62}$$

$$= \mathbb{E}\left[\sum_{(r,s)\in\mathcal{N}^2}\sum_{\phi=1}^{\Phi} e_{rs}^{\phi}(t)\middle|\mathbf{e}(t)\right] \tag{63}$$

$$= \mathbb{E}\left[\sum_{(r,s)\in\mathcal{N}^2}\sum_{\phi=1}^{\Phi}\left(w_{rs}^{\phi}(t) - w_{rs}^{\phi+1}(t+1) - \sum_{q\in\mathcal{N}} v_{qrs}^{\phi}(t)\right)\middle|\mathbf{w}(t)\right] \tag{64}$$

$$\leq \mathbb{E}\left[\sum_{(r,s)\in\mathcal{N}^2}\sum_{\phi=1}^{\Phi} w_{rs}^{\phi}(t)\,\middle|\,\mathbf{w}(t)\right] \tag{65}$$

$$= \sum_{(r,s)\in\mathcal{N}^2}\left(\Phi\hat{d}_{rs}\right) \tag{66}$$

■

Lemma 4.3: *When policy $\pi^\star$ is used and $\bar{\mathbf{d}} \in \mathcal{D}^0$, with exiting passengers $\mathbf{e}(t)$ at each time step, there exists a Lyapunov function $\nu(t) \geq 0$ and constants $\kappa < \infty, \epsilon > 0$ such that*

$$\mathbb{E}\left[\nu(t+1) - \nu(t)|\,\omega(t)\right] \leq \kappa - \epsilon\omega(t) \tag{67}$$

Proof: Consider the following Lyapunov function, which includes the waiting passengers $w_{rs}(t)$ and exiting passengers $e_{rs}(t)$.

$$\nu(t) = \omega(t)\left(\sum_{(r,s)\in\mathcal{N}^2}\sum_{\phi=1}^{\Phi}\bar{C}_{rs}w_{rs}^{\phi}(t)\right) + \omega(t)\left(\sum_{s\in\mathcal{N}}\sum_{\tau=1}^{\infty}\tau x_s^{\tau}(t)\right) \tag{68}$$

For ease of presentation, define $\nu(t) = \nu_1(t) + \nu_2(t)$ where

$$\nu_1(t) = \omega(t)\left(\sum_{(r,s)\in\mathcal{N}^2}\sum_{\phi=1}^{\Phi}\bar{C}_{rs}w_{rs}^{\phi}(t)\right) \tag{69}$$

and

$$\nu_2(t) = \omega(t)\left(\sum_{s\in\mathcal{N}}\sum_{\tau=1}^{\infty}\tau x_s^{\tau}(t)\right) \tag{70}$$

First, we expand the difference $\nu_1(t+1) - \nu_1(t)$. Then

$$\begin{aligned}\nu_1(t+1) - \nu_1(t) &= \omega(t+1)\left(\sum_{(r,s)\in\mathcal{N}^2}\sum_{\phi=1}^{\Phi}\bar{C}_{rs}w_{rs}^{\phi+1}(t+1)\right)\\ &\quad - \omega(t)\left(\sum_{(r,s)\in\mathcal{N}^2}\sum_{\phi=1}^{\Phi}\bar{C}_{rs}w_{rs}^{\phi}(t)\right) \qquad (71)\\ &= (\omega(t+1) - \omega(t) + \omega(t))\left(\sum_{(r,s)\in\mathcal{N}^2}\sum_{\phi=1}^{\Phi}\bar{C}_{rs}w_{rs}^{\phi+1}(t+1)\right)\\ &\quad - \omega(t)\left(\sum_{(r,s)\in\mathcal{N}^2}\sum_{\phi=1}^{\Phi}\bar{C}_{rs}w_{rs}^{\phi}(t)\right) \qquad (72)\end{aligned}$$

$$= (\omega(t+1) - \omega(t)) \left(\sum_{(r,s)\in\mathcal{N}^2} \sum_{\phi=1}^{\Phi} \bar{C}_{rs} \left(w_{rs}^{\phi+1}(t+1) \right) \right)$$
$$+ \omega(t) \left(\sum_{(r,s)\in\mathcal{N}^2} \sum_{\phi=1}^{\Phi} \bar{C}_{rs} (w_{rs}^{\phi+1}(t+1) - w_{rs}^{\phi}(t)) \right) \tag{73}$$

$\mathbb{E}\left[(\omega(t+1) - \omega(t)) (\sum_{(r,s)\in\mathcal{N}^2} \sum_{\phi=1}^{\Phi} \bar{C}_{rs} (w_{rs}^{\phi+1}(t+1))) \right]$ is bounded based on Lemmas 4.1 and 4.2. We leave the second term for later. Now we continue working with $\nu_2(t+1) - \nu_2(t)$.

$$\nu_2(t+1) - \nu_2(t)$$
$$= \omega(t+1) \left(\sum_{s\in\mathcal{N}} \sum_{\tau=1}^{\infty} \tau x_s^{\tau}(t+1) \right) - \omega(t) \left(\sum_{s\in\mathcal{N}} \sum_{\tau=1}^{\infty} \tau x_s^{\tau}(t) \right) \tag{74}$$
$$= (\omega(t+1) - \omega(t) + \omega(t)) \left(\sum_{s\in\mathcal{N}} \sum_{\tau=1}^{\infty} \tau x_s^{\tau}(t+1) \right) - \omega(t) \left(\sum_{s\in\mathcal{N}} \sum_{\tau=1}^{\infty} \tau x_s^{\tau}(t) \right) \tag{75}$$
$$= (\omega(t+1) - \omega(t))) \left(\sum_{s\in\mathcal{N}} \sum_{\tau=1}^{\infty} \tau (x_s^{\tau}(t+1)) \right) + \omega(t) \left(\sum_{s\in\mathcal{N}} \sum_{\tau=1}^{\infty} \tau (x_s^{\tau}(t+1) - x_s^{\tau}(t)) \right) \tag{76}$$

The first term of Equation (76) is still bound because of Lemma 4.2 and $\sum_{\tau=0}^{\infty} x_s^{\tau}(t) = F$. Note that the maximum travel time is still bound although we use ∞ here instead of defining the maximum.

After that, we combine $\nu_1(t+1) - \nu_1(t)$ and $\nu_2(t+1) - \nu_2(t)$.

$$\begin{aligned}
\nu(t+1) - \nu(t) &= (\nu_1(t+1) + \nu_2(t+1)) - (\nu_1(t) - \nu_2(t)) \\
&= \nu_1(t+1) - \nu_1(t) + \nu_2(t+1) - \nu_2(t) \\
&= (\omega(t+1) - \omega(t)) \left(\sum_{(r,s)\in\mathcal{N}^2} \sum_{\phi=1}^{\Phi} \bar{C}_{rs} \left(w_{rs}^{\phi+1}(t+1) \right) \right) \\
&\quad + \omega(t) \left(\sum_{(r,s)\in\mathcal{N}^2} \sum_{\phi=1}^{\Phi} \bar{C}_{rs} (w_{rs}^{\phi+1}(t+1) - w_{rs}^{\phi}(t)) \right) \\
&\quad + (\omega(t+1) - \omega(t)) \left(\sum_{s\in\mathcal{N}} \sum_{\tau=1}^{\infty} \tau (x_s^{\tau}(t+1) \right) \\
&\quad + \omega(t) \left(\sum_{s\in\mathcal{N}} \sum_{\tau=1}^{\infty} \tau (x_s^{\tau}(t+1) - x_s^{\tau}(t)) \right)
\end{aligned} \tag{77}$$

Based on Lemma 4.1 and 4.2, $\mathbb{E}\left[(\omega(t+1) - \omega(t)) (\sum_{(r,s)\in\mathcal{N}^2} \sum_{\phi=1}^{\Phi} \bar{C}_{rs} (w_{rs}^{\phi+1}(t+1))) \right]$ is bounded by $\sum_{(r,s)\in\mathcal{N}^2} (\Phi \hat{d}_{rs}) \bar{C}_{rs} (\Phi \hat{d}_{rs})$. Because we know $\sum_{\tau=1}^{\infty} x_s^{\tau}(t+1) \leq F$, term

$\mathbb{E}\left[(\omega(t+1)-\omega(t))(\sum_{s\in\mathcal{N}}\sum_{\tau=1}^{\infty}\tau(x_s^\tau(t+1))\right]$ is bounded by $\sum_{(r,s)\in\mathcal{N}^2}(\Phi\hat{d}_{rs})\times(F\times\max_{(q,r,s)\in\mathcal{N}^3}\{C_{qrs}\})$. We can obtain the following equation:

$$\begin{aligned}\nu(t+1)-\nu(t)\leq&\left[\sum_{(r,s)\in\mathcal{N}^2}\left(\Phi\hat{d}_{rs}\right)\bar{C}_{rs}\left(\Phi\hat{d}_{rs}\right)\right]+\left(\Phi\hat{d}_{rs}\right)\times\left(F\times\max_{(q,r,s)\in\mathcal{N}^3}\left\{C_{qrs}\right\}\right)\\&+\omega(t)\Bigg[\left(\sum_{(r,s)\in\mathcal{N}^2}\sum_{\phi=1}^{\Phi}\bar{C}_{rs}(w_{rs}^{\phi+1}(t+1)-w_{rs}^{\phi}(t))\right)\\&+\left(\sum_{s\in\mathcal{N}}\sum_{\tau=1}^{\infty}\tau(x_s^\tau(t+1)-x_s^\tau(t)\right)\Bigg]\end{aligned}\tag{78}$$

We now consider the third term of the above equation:

$$\begin{aligned}\mathbb{E}\Bigg[\omega(t)\Bigg(&\left(\sum_{(r,s)\in\mathcal{N}^2}\sum_{\phi=1}^{\Phi}\bar{C}_{rs}(w_{rs}^{\phi+1}(t+1)-w_{rs}^{\phi}(t))\right)\\&+\left(\sum_{s\in\mathcal{N}}\sum_{\tau=1}^{\infty}\tau(x_s^\tau(t+1)-x_s^\tau(t))\right)\Bigg)\Bigg|\sum_{t'=1}^{t}\mathbf{e}(t),\mathbf{w}(t),\mathbf{x}(t)\Bigg]\end{aligned}\tag{79}$$

Based on Equation (47), we sum all waiting passengers from $\phi=0$ to $\phi=\Phi$ at time t, $(\sum_{\phi=1}^{\Phi}(w_{rs}^{\phi+1}(t+1)-w_{rs}^{\phi}(t)))$ in Equation (79) can be rewritten as follows

$$\sum_{\phi=0}^{\Phi}w_{rs}^{\phi+1}(t+1)=\sum_{\phi=0}^{\Phi}w_{rs}^{\phi}(t)-\sum_{\phi=0}^{\Phi}e_{rs}^{\phi}(t)-\sum_{q\in\mathcal{N}}\sum_{\phi=0}^{\Phi}v_{qrs}(t)\tag{80}$$

Equation (80) can be rewritten as

$$\sum_{\phi=1}^{\Phi}w_{rs}^{\phi+1}(t+1)+w_{rs}^{1}(t+1)=\sum_{\phi=1}^{\Phi}w_{rs}^{\phi}(t)+w_{rs}^{0}(t)-\sum_{\phi=0}^{\Phi}e_{rs}^{\phi}(t)-\sum_{q\in\mathcal{N}}\sum_{\phi=0}^{\Phi}v_{qrs}^{\phi}(t)\tag{81}$$

Since $e_{rs}^{0}(t)=0$ and $w_{rs}^{0}(t)=d_{rs}(t)$, we have the following equation

$$\sum_{\phi=1}^{\Phi}w_{rs}^{\phi+1}(t+1)+w_{rs}^{1}(t+1)=\sum_{\phi=1}^{\Phi}w_{rs}^{\phi}(t)+d_{rs}(t)-\sum_{\phi=1}^{\Phi}e_{rs}^{\phi}(t)-\sum_{q\in\mathcal{N}}\sum_{\phi=0}^{\Phi}v_{qrs}^{\phi}(t)\tag{82}$$

Moving on, we have

$$\sum_{\phi=1}^{\Phi}w_{rs}^{\phi+1}(t+1)-\sum_{\phi=1}^{\Phi}w_{rs}^{\phi}(t)=d_{rs}(t)-\sum_{\phi=1}^{\Phi}e_{rs}^{\phi}(t)-\sum_{q\in\mathcal{N}}\sum_{\phi=0}^{\Phi}v_{qrs}^{\phi}(t)-w_{rs}^{1}(t+1)\tag{83}$$

Combining Equations (79) and (83) yields

$$\mathbb{E}\Bigg[\omega(t)\left(\sum_{(r,s)\in\mathcal{N}^2}\bar{C}_{rs}\left(d_{rs}(t)-\sum_{\phi=1}^{\Phi}e_{rs}^{\phi}(t)-\sum_{\phi=0}^{\Phi}\sum_{q\in\mathcal{N}}v_{qrs}^{\phi}(t)-w_{rs}^{1}(t+1)\right)\right)$$
$$-\left(\sum_{s\in\mathcal{N}}\sum_{\tau=1}^{\infty}\tau(x_s^{\tau}(t+1)-x_s^{\tau}(t))\right)\Bigg|\sum_{t'=1}^{t}\mathbf{e}(t),\mathbf{w}(t),\mathbf{x}(t)\Bigg] \tag{84}$$

Let us focus on the term $(\sum_{s\in\mathcal{N}}\sum_{\tau=1}^{\infty}\tau(x_s^{\tau}(t+1)-x_s^{\tau}(t)))$ of Equations (78), (79) and (84), which satisfies the same derivation as Equations (35) to (38). We can get $(\sum_{s\in\mathcal{N}}\sum_{\tau=1}^{\infty}\tau(x_s^{\tau}(t+1)-x_s^{\tau}(t)))=-F+\sum_{(q,r,s)\in\mathcal{N}^3}v_{qrs}(t)C_{qrs}$. Therefore, Equation (79), which is also the third term of (78), can be rewritten as follows

$$\mathbb{E}\Bigg[\omega(t)\left(\sum_{(r,s)\in\mathcal{N}^2}\bar{C}_{rs}\left(d_{rs}(t)-\sum_{\phi=1}^{\Phi}e_{rs}^{\phi}(t)-\sum_{\phi=0}^{\Phi}\sum_{q\in\mathcal{N}}v_{qrs}^{\phi}(t)-w_{rs}^{1}(t+1)\right)\right)$$
$$-\left(F+\sum_{(q,r,s)\in\mathcal{N}^3}v_{qrs}(t)C_{qrs}\right)\Bigg|\sum_{\phi=1}^{\Phi}\mathbf{e}(t),\mathbf{w}(t)\Bigg] \tag{85}$$

Because policy $\pi^{\star}$ is used, $v_{qrs}^{\star}(t)$ will be chosen by the policy. and the dispatched vehicle by policy $\pi^{\star}$ at time step t satisfies Equation (53) .Therefore we have the inequality $\sum_{q\in\mathcal{N}}\sum_{\phi=0}^{\Phi}v_{qrs}^{\phi}(t)C_{qrs}=\sum_{(q,r,s)\in\mathcal{N}^3}v_{qrs}^{\star}(t)C_{qrs}\le\sum_{(q,r,s)\in\mathcal{N}^3}\bar{v}_{qrs}C_{qrs}=\sum_{(q,r,s)\in\mathcal{N}^3}\bar{v}_{qrs}\bar{C}_{rs}$. Now we can reform Equation (85) based on the proposed policy.

$$\begin{aligned}
&\mathbb{E}\Bigg[\omega(t)\left(\sum_{(r,s)\in\mathcal{N}^2}\bar{C}_{rs}\left(d_{rs}(t)-\sum_{\phi=1}^{\Phi}e_{rs}^{\phi}(t)-\sum_{q\in\mathcal{N}}\sum_{\phi=0}^{\Phi}v_{qrs}^{\phi}(t)-w_{rs}^{1}(t+1)\right)\right)\\
&\quad-\left(F+\sum_{(q,r,s)\in\mathcal{N}^3}\sum_{\phi=0}^{\Phi}v_{qrs}^{\phi}(t)C_{qrs}\right)\Bigg|\sum_{\phi=1}^{\Phi}\mathbf{e}(t),\mathbf{w}(t)\Bigg]\\
&\le\mathbb{E}\left[\omega(t)\left(\sum_{(r,s)\in\mathcal{N}^2}\bar{C}_{rs}\left(d_{rs}(t)-\sum_{\phi=1}^{\Phi}e_{rs}^{\phi}(t)-\sum_{q\in\mathcal{N}}\sum_{\phi=0}^{\Phi}v_{qrs}^{\phi}(t)\right)\right)\Bigg|\sum_{\phi=1}^{\Phi}\mathbf{e}\right](t)\\
&\le\mathbb{E}\left[\omega(t)\left(-F+\sum_{(r,s)\in\mathcal{N}^2}\bar{C}_{rs}\left(d_{rs}(t)-\sum_{\phi=1}^{\Phi}e_{rs}(t)\right)\right)\Bigg|\sum_{\phi=1}^{\Phi}\mathbf{e}(t)\right]
\end{aligned} \tag{86}$$

Based on the definition of the stable region with exiting passengers, we have the relationship of Equations (50), (55) and (56). Therefore, Equation (86) can be rewritten as

follows:

$$\mathbb{E}\left[\omega(t)\left(-F+\sum_{(r,s)\in\mathcal{N}^2}\bar{C}_{rs}\left(d_{rs}(t)-\sum_{\phi=1}^{\Phi}e_{rs}^{\phi}(t)\right)\right)\mid\sum_{\phi=1}^{\Phi}\mathbf{e}(t),\mathbf{x}(t)\right]$$

$$\leq\left(\sum_{(q,r,s)\in\mathcal{N}^3}\bar{v}_{qrs}C_{qrs}-F\right)\omega(t) \tag{87}$$

$$=-\epsilon|\boldsymbol{\omega}(t)| \tag{88}$$

Looking back to the first and second terms of Equation (78). We find they are bounded by constant by $\kappa_1=[\sum_{(r,s)\in\mathcal{N}^2}(\Phi\hat{d}_{rs})\bar{C}_{rs}(\Phi\hat{d}_{rs})]$ and $\kappa_2=(\Phi\hat{d}_{rs})\times(F\times\max_{(q,r,s)\in\mathcal{N}^3}\{C_{qrs}\})$ respectively, so there exists a constant $\kappa=(\kappa_1+\kappa_2)<\infty$ and a constant $\epsilon>0$ from Equation (88) that makes function $v(t)=\omega(t)(\sum_{(r,s)\in\mathcal{N}^2}\sum_{\phi=1}^{\Phi}\bar{C}_{rs}w_{rs}^{\phi}(t))+\omega(t)(\sum_{s\in\mathcal{N}}\sum_{\tau=1}^{\infty}\tau x_s^{\tau}(t))$ that satisfies the inequality (67), $\mathbb{E}[v(t+1)-v(t)|\omega(t)]\leq\kappa-\epsilon\omega(t)$. ■

Proposition 4.1: *When policy $\pi^\star$ is used and $\bar{\mathbf{d}}\in\mathcal{D}^0$, the network is stable.*

Proof: Inequality (67) holds from Lemma 4.3. Taking expectations and summing over $t=1,\ldots,T$ gives the following inequality:

$$\mathbb{E}[v(T+1)-v(1)|\,\omega(t)]\leq\kappa T-\epsilon\sum_{t=1}^{T}\omega(t) \tag{89}$$

and so,

$$\epsilon\frac{1}{T}\sum_{t=1}^{T}\mathbb{E}[\omega(t)]\leq\kappa-\frac{1}{T}\mathbb{E}[v(T+1)]+\frac{1}{T}\mathbb{E}[v(1)]\leq\kappa+\frac{1}{T}\mathbb{E}[v(1)] \tag{90}$$

We move ϵ to the right-hand side and take the limit as T goes to infinity. Then the $\frac{1}{T}\mathbb{E}[v(1)]$ term approaches zero, which yields

$$\lim_{T\to\infty}\frac{1}{T}\sum_{t=1}^{T}\mathbb{E}[\omega(t)]\leq\frac{\kappa}{\epsilon} \tag{91}$$

Note that Equation (91) can be rewritten as follows:

$$\lim_{T\to\infty}\frac{1}{T}\mathbb{E}\left[\sum_{t=1}^{T}\omega(t)\right]\leq\frac{\kappa}{\epsilon} \tag{92}$$

$$\lim_{T\to\infty}\frac{1}{T}\mathbb{E}\left[\underbrace{\omega(1)+\omega(2)+\cdots+\omega(T)}_{T}\right]\leq\frac{\kappa}{\epsilon} \tag{93}$$

$$\lim_{T\to\infty}\frac{1}{T}\mathbb{E}[T\times\mathbb{E}[\omega(T)]]\leq\frac{\kappa}{\epsilon} \tag{94}$$

Moving T to the right hand side of Equation (94), we have

$$\lim_{T\to\infty}\frac{1}{T}\mathbb{E}[\omega(T)]\leq\frac{\kappa}{\epsilon T} \tag{95}$$

When T approaches infinity, the right-hand side of Equation (95) approaches zero, which is equivalent to Equation (52). Therefore, Definition 4.1 is satisfied. ■

5. Simulation model and numerical results

We use the Sioux Falls network, which includes 24 nodes and 72 links, to provide numerical analysis for the proposed maximum-stability dispatch policy for SAVs. It has been used quite often in the literature as a benchmark. The total demand is around 360600 trips per day (around 15025 trips per hour). The main purpose of the simulation is to numerically demonstrate the stability properties discussed in previous sections. The simulation experiments are built in Java, and the optimisation programmes are solved in IBM CPLEX. We set the simulation to 1500 time steps (45000 seconds in reality) to ensure it is enough long for stability. Each time step equals 30 seconds in this simulation.

The simulation and numerical analysis are divided into three parts. The first is the maximum-stability applied when there are no exiting passengers, which we called basic simulation and stability analysis. The second part is a small example, which explains the impacts of fleet size on maximum stable demand. It can help readers better understand the results of the experiment. The third part is about extending the simulation stability analysis to consider the exiting passengers.

5.1. Basic simulation and stability analysis

In this part, we first show the numerical difference in the average queue length of waiting for passengers inside and outside the stable region when the fleet size is 450 vehicles. The average queue length of waiting for passengers is defined as the number of waiting for passengers that are waiting to be picked up by SAVs. This number is summed over all zones and averaged by the simulation time. The results are shown in Figure 2, which shows that for stable demand, the average queue length of waiting passengers will approach to a constant, while for unstable demand, the average queue length of waiting passengers will increase to an arbitrarily large number.

Similarly, we also show the numerical difference in average passenger waiting time with a fleet of 450 vehicles in Figure 3. The average passenger waiting time is calculated by summing up all served waiting passengers, and average over the simulation time and the number of served waiting passengers. The average queue length of waiting passengers is calculated by summing all served passenger waiting time, averaged over simulation time. Therefore, according to Little's Law, average passenger waiting time will have the same pattern shown in Figure 2. The results are shown in Figure 3, which shows that for a stabilisable demand, the average passenger waiting time will fluctuate around a constant number, while for unstabilisable demand, the average passenger waiting time will increase to infinity. Readers may notice from Figures 2 and 3, the time that required to converge to a constant is different when different indicators are considered. However, there is no theoretical reason why the average waiting time and the average waiting passengers should have the same pattern in the simulation. With a sufficiently long time horizon, they will both converge to average values for a stable network, but there is no theoretical relationship between when they converge.

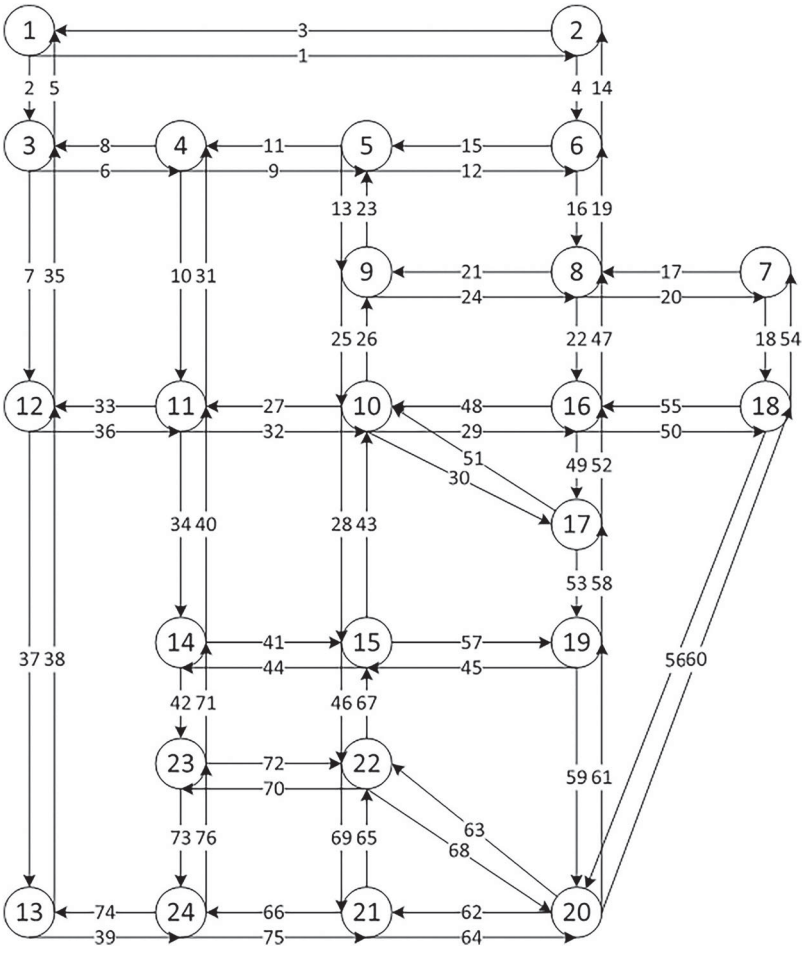

Figure 1. Sioux falls network.

We also find when the demand is within the stable region, the average empty vehicle travel time will fluctuate around a constant when the fleet size is 450 vehicles. However, when the demand is outside the stable region, the average empty vehicle travel time will continually increase to a number then drop to a constant. Finally, the average empty vehicle travel time will fluctuate around a constant too. This is because, when the queue of passengers is increasing in length, there is likely to be at least one passenger waiting to be picked up at each node each time step. As time goes on, an increased number of unserved passengers accumulates at each node, a vehicle will most likely be able to pick up a passenger at the same node where it drops a passenger off at. This results in zero empty travel time steps for some vehicle's trips. As a result, the average empty travel time will approach a constant. Note that the proportion of vehicles that has zero empty vehicle travel time in the fleet size should depend on how much passenger demand exceeds the stable demand region. If the demand is too large, the average empty vehicle travel time will converge to zero since more vehicles will pick up and drop off passengers at the same nodes.

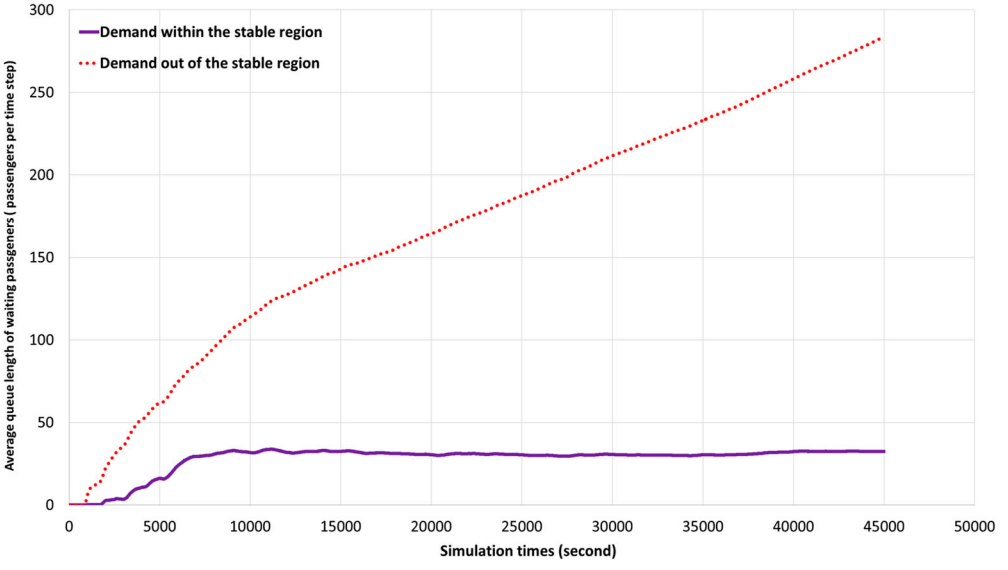

Figure 2. Difference in the average queue length of waiting passengers for demand inside and outside the stable region.

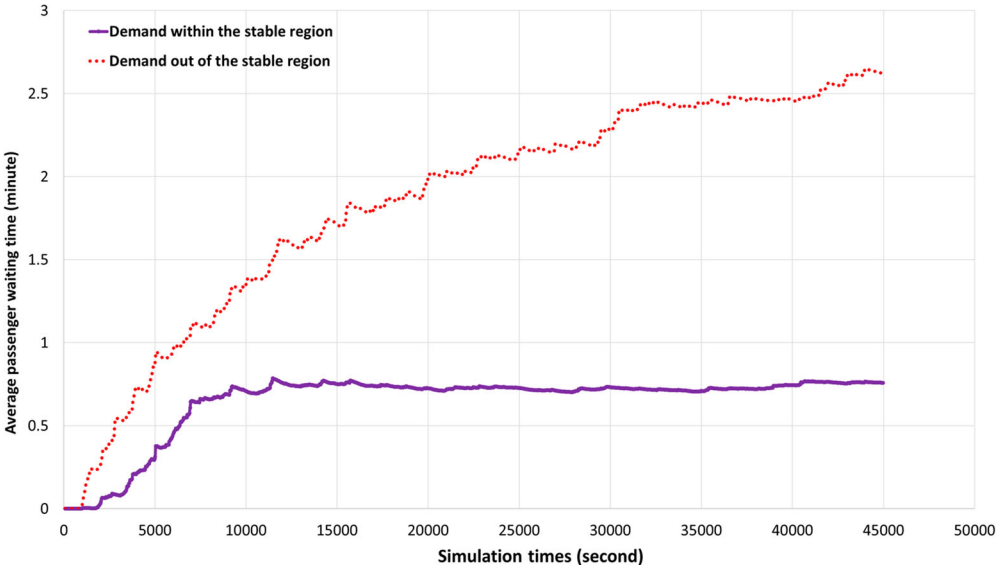

Figure 3. Difference in the average passenger waiting time for demand inside and outside the stable region.

Figure 5 plots the average passenger waiting time with regard to fleet size when the total demand is 15025 trips per day. The results show that when the fleet size increase from 250 to 650 vehicles, the average passenger waiting time shows a decreasing trend when the demand is within the stable region in this network.

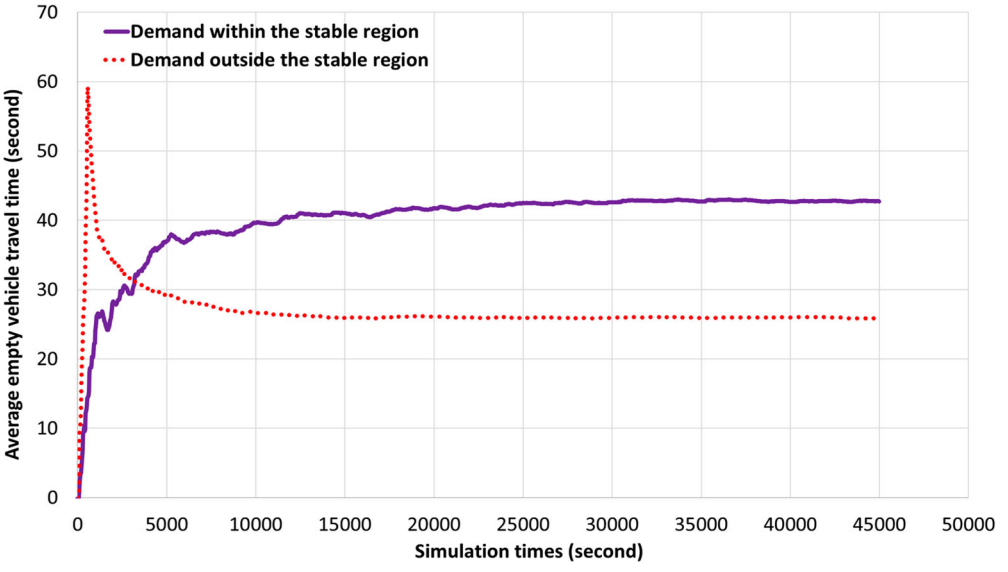

Figure 4. Difference in the average empty vehicle travel time for demand inside and outside the stable region.

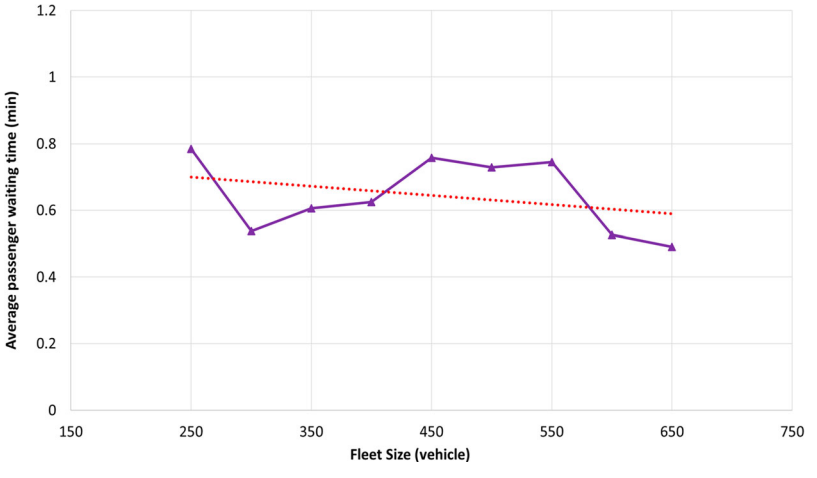

Figure 5. Average passenger waiting time with respect to different fleet sizes under stable demand.

5.2. Impact of fleet size on maximum stable demand

The maximum trips per hour of SAVs calculated by simulation under the stable region with different fleet sizes are shown in Figure 6. When the fleet size increases from 250 vehicles to 650 vehicles, maximum trips per hour of SAVs increases linearly with respect to fleet size. The dashed line in Figure 6 shows the maximum trips per hour calculated by Equations (8), (9) and (12). When fleet size increases from 250 vehicles to 650 vehicles, the maximum trips per hour of SAVs solved by the equations characterising the stable region also increases linearly with respect to fleet size. However, the simulation-based maximum trips per hour is smaller compared with maximum trips per hour predicted by Equations (8), (9)

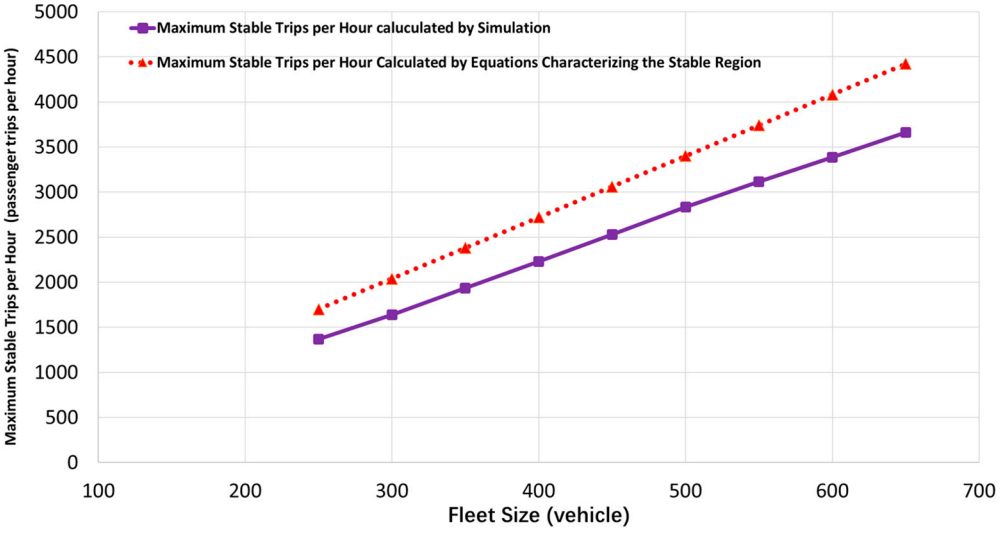

Figure 6. Trips per hour with regard to different fleet sizes under stable demand.

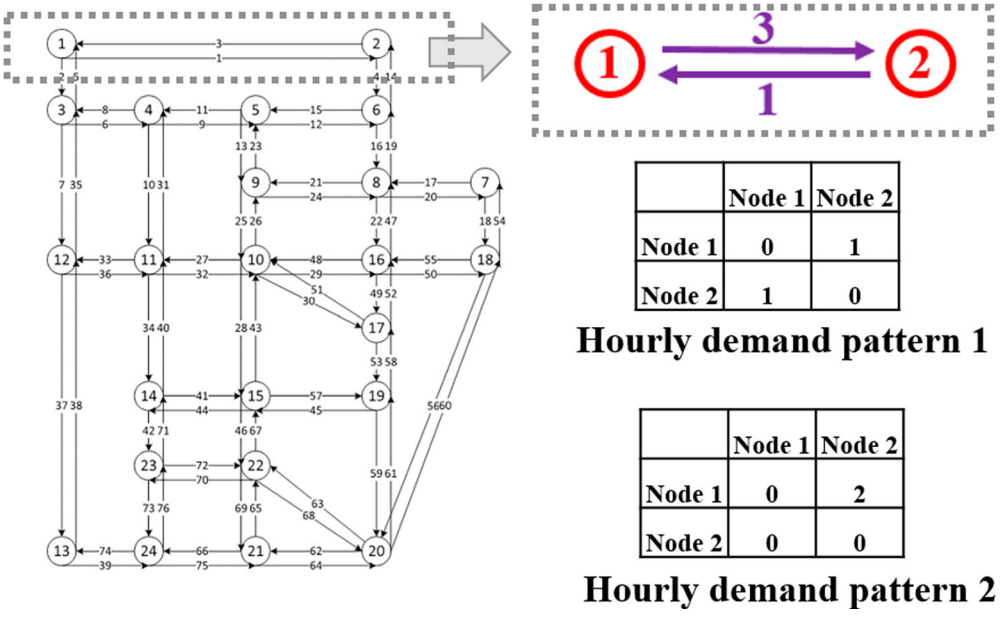

Figure 7. Small network.

and (12). Specifically, these results may provide practical applications for SAVs. For example, SAV companies could use the maximum stability dispatch policy to choose the number of vehicles to operate within one city to both satisfy traveller demand and ensure low waiting times. SAV companies can also make an informed decision to balance SAV trips per hour with vehicle fleet size to optimise operating costs.

We notice that maximum stable demand per hour within the stable region with respect to different fleet sizes is smaller than the maximum stable demand per hour predicted by

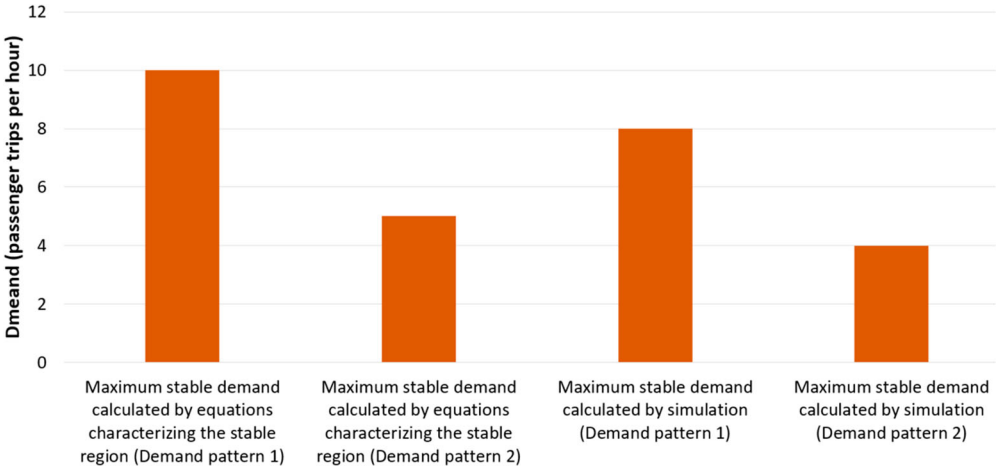

Figure 8. Experimental results of the small network.

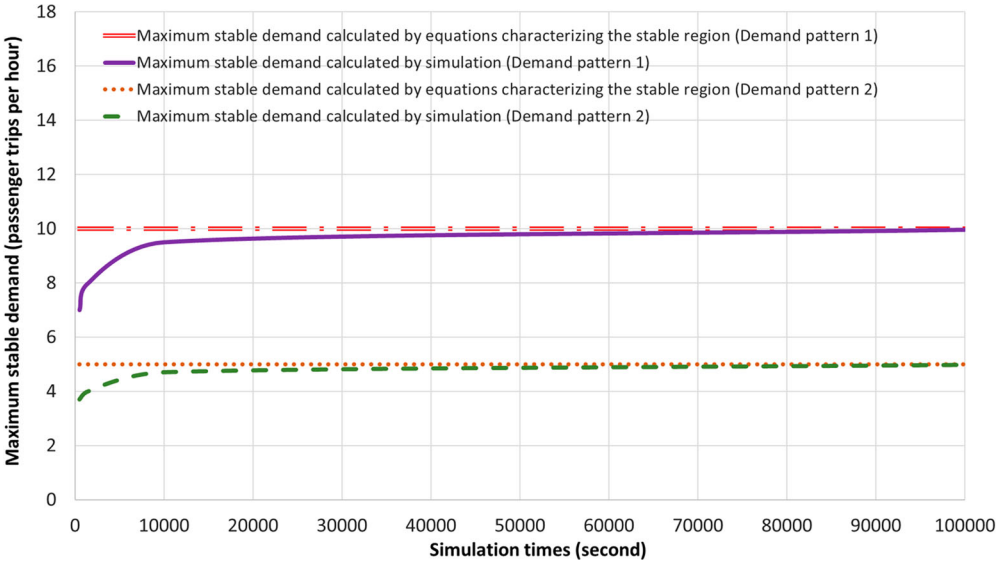

Figure 9. Maximum stable demand results with respect to simulation horizons.

solving Equations (8), (9) and (12). Based on Equations (8), (9) and (12), we can analytically predict the maximum stable demand per hour based on the given fleet size and the demand file of the Sioux Falls Network. But when running the simulation, we find there is some difference between simulation-based results and analytically solved results, as shown in Figure 6.

We use a small network, which only includes node 1, node 2, link 1, and link 3 in the Sioux Falls Network, to explain the difference, as shown in Figure 6. The shortest path travel time between node 1 and node 2 is 6 minutes, and the shortest path travel time between node 2 and node 1 is also 6 minutes. We set the demand between these two nodes as 2 trips per hour the fleet size is one. In addition, we need to emphasise a small network with one

SAV can help us understand how the vehicle moves between the only two nodes. The reason we use a small demand is that we need to simulate a long time horizon and a smaller demand will reduce the computation time. We set two small demand patterns. Pattern 1 is symmetric, which means the hourly trips between node 1 to node 2 is 1, and the hourly trips between node 2 to node 1 is 1 too. Pattern 2 is asymmetric: the hourly trips between node 1 to node 2 are 2, but the hourly trip between node 2 to node 1 is zero. For the small network, the SAV fleet size (one SAV) can make 5 round trips per hour. For pattern 1, each round trip serves 2 passengers. Therefore, the SAV fleet (one SAV) can serve a maximum of 10 passengers per hour. For pattern 2, each round trip serves 1 passenger. Therefore, this SAV fleet (one SAV) can serve a maximum of 5 passengers per hour. This is reasonable, because when the demand pattern is asymmetric, SAVs need rebalancing trips, which makes the shortest path travel time larger. We also set the two small demand patterns into the simulation and we find the maximum stable demands are different under these two demand patterns. Under the small demand pattern 1 (symmetric), the maximum stable demand calculated by simulation is around 8 trips per hour. Under the small demand pattern 1 (symmetric), the maximum stable demand calculated by simulation is around 4 trips per hour. This is reasonable because SAVs also need rebalancing trips in simulations. The results are shown in Figure 6, which demonstrates that the demand distribution influences the maximum stable demand. However, Equations (8), (9) and (12) consider asymmetric trips.

Moving on, we set the simulation time horizon from 1000 to 100,000 to check the impacts on the maximum stable demand. Figure 6 shows that the gap between simulation results and the results calculated from Equations (8), (9) and (12) decreases as the simulation time horizons increase, which demonstrates our simulation is exactly matched with the results calculated from Equations (8), (9) and (12) if we choose sufficiently large simulation time horizons. The reason for the above-mentioned relationship between gap and simulation step horizons is that when we set up a larger demand, the ϵ in Equation (16) becomes smaller based on a given fleet size, which makes the upper bound of Equation (5) larger. Therefore, it requires a larger simulation time horizon to converge to this larger upper bound.

5.3. Simulation and stability analysis including exiting passengers

Using the same demand as in Section 5.1, we extend our simulation to consider the existence of exiting passengers. First, we show the numerical difference in the average cumulative unserved passengers inside and outside of the stable region when the fleet size is 450 vehicles and the waiting tolerance time is 5, 10, and 15 minutes. The waiting tolerance time means the largest waiting time that passengers are willing to wait. The average cumulative unserved passengers are defined in Definition 4.1. To ensure we can observe more evolutionary detail of stability from the simulation, we set the simulation times sufficiently large. Figure 10 shows that for stable demand, the average cumulative unserved passengers fluctuates around a constant close to zero under the three different tolerance times. However, for unstable demand, the average cumulative unserved passengers fluctuates around a number significantly larger than 0. Figure 10 also indicates that, based on the same unstable demand, the smaller tolerance time leads to a larger average cumulative number of unserved passengers. This is true because when the tolerance time is smaller, passengers will choose to leave the queue earlier. Based on the same stable demand, the

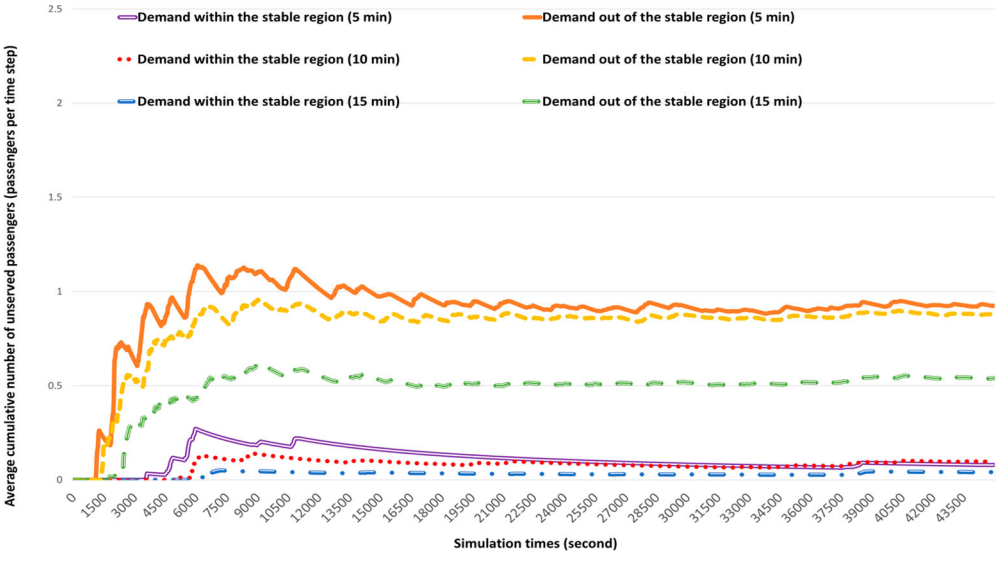

Figure 10. Difference in the average number of unserved passengers for demand inside and outside the stable region.

average cumulative number of unserved passengers is larger when the tolerance time is small at the beginning, but this number will converge to a very small number (close to zero) as the simulations continue.

We also show the numerical difference in the average queue length of waiting passengers inside and outside the stable region when considering exiting passengers with different tolerance times. The fleet size is also 450 SAVs. The results are shown in Figure 11. Because of the tolerance time, people will leave the system if their waiting times are longer than they can tolerate, which means the average queue length for the unstable network will also be bound. Note that a stable and unstable network is defined by the average cumulative number of unserved passengers when considering exiting passengers, not the average queue length. As for stable demand and unstable demand, when the tolerance time increases, the average queue length of waiting passengers increases too.

Figure 12 shows the numerical difference in the waiting time of waiting passengers inside and outside the stable region when considering the exiting passengers with different tolerance time. Based on Little's Law, the average passenger waiting times have same the pattern as shown in Figure 12.

Average empty vehicle travel times are also worth exploring when considering the exiting passengers. The results are shown in Figure 13. When the demand is within the stable region, the average empty vehicle travel time will fluctuate around a constant under different tolerance times. When the demand is out of the stable region, the average empty vehicle travel time will also fluctuate around a constant when the demand is out of the stable region. This is because when considering tolerance times of exiting passengers, all non-exiting passengers will be served by SAVs, which makes the number of waiting passengers in the queue will be bound. Finally, the average empty vehicle travel time will converge to a constant.

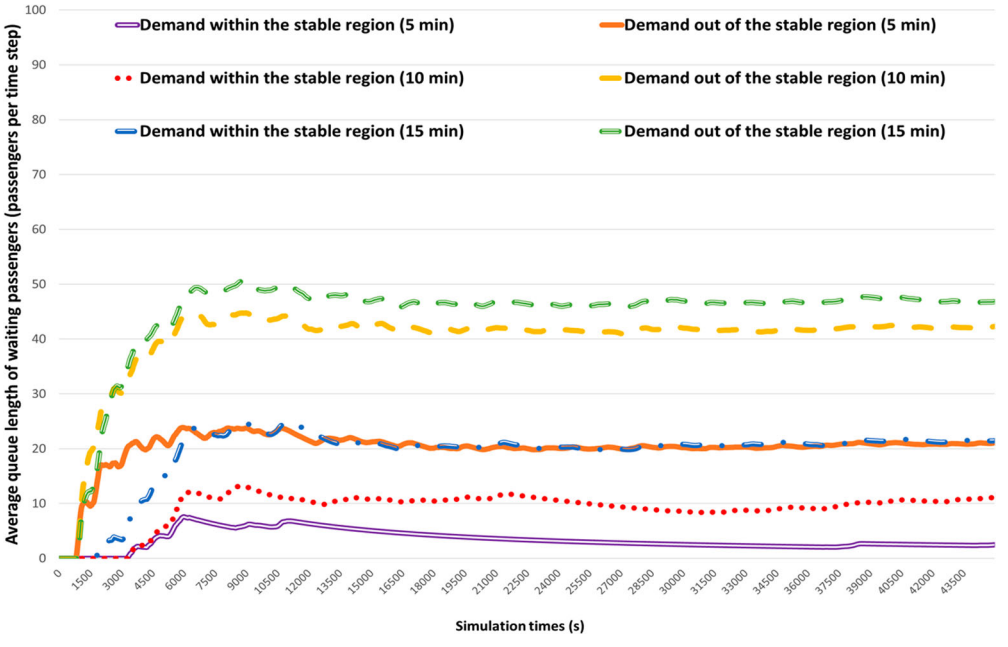

Figure 11. Difference in the average queue length of waiting passengers for demand inside and outside the stable region.

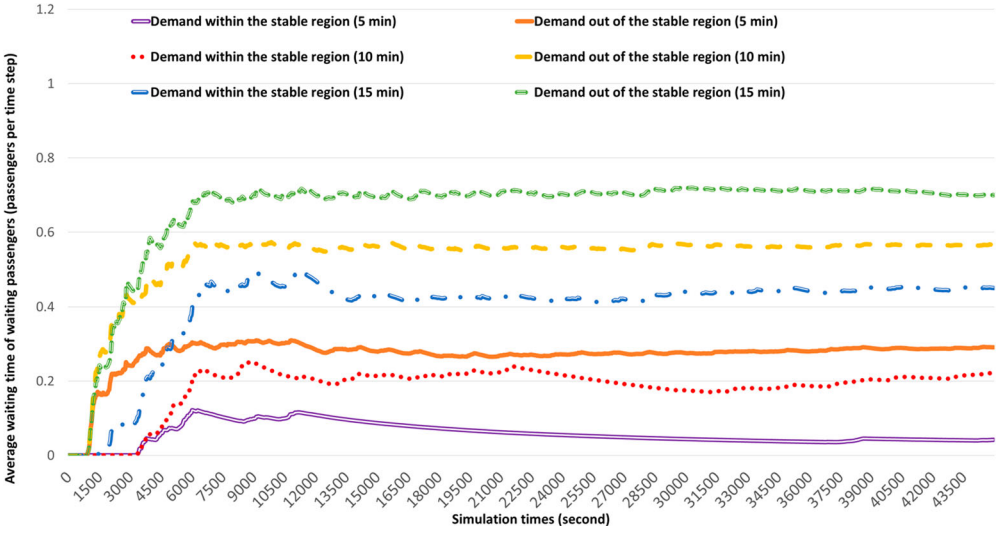

Figure 12. Difference in the average waiting time of waiting passengers for demand inside and outside the stable region.

The maximum trips per hour of SAVs calculated by simulations under the stable region with different fleet sizes with exiting passengers (tolerance time: 10 minutes) are shown in Figure 14. When considering exiting passengers, the maximum trips per hour of SAVs increase linearly with respect to different fleet sizes. Furthermore, the results show that the

Figure 13. Difference in empty vehicle travel time for demand inside and outside the stable region.

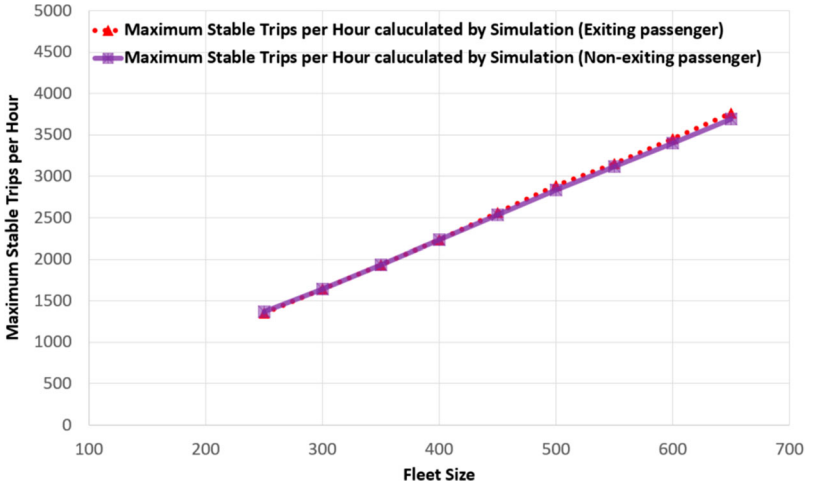

Figure 14. Trips per hour with regard to different fleet size under stable demand when considering exiting passengers.

exiting passengers do not affect the stable region. When the demand is within the stable region, the average number of exiting passengers will reach nearly zero. Therefore, the maximum stable region is the same with or without exiting passengers. This is consistent with the results of Figure 10. Both Figures 10 and 14 give us the insight that a particular fleet size is needed to serve a given passenger regardless of whether passengers exit due to long waiting times. In other words, if the SAV operator wants to provide a stable service, the fleet size can be the same under with or without exiting passengers.

6. Conclusions

This study develops a fast maximum stability dispatch policy, named FMS-Dispatch, for SAVs based on the dynamic queueing model. We characterise the stable region, which is the set of demands that could be served by any dispatch policy. Based on the simulation results, we find the results numerically show that the proposed fast maximum-stability dispatch policy can ensure that the network remains stable when stochastic demand is within the stable region. Furthermore, the numerical results show that the maximum stable demand per hour of SAVs increases linearly with respect to the fleet size. We also find that an asymmetrical demand pattern will add rebalancing time for SAVs, which can lead to the maximum stable demand per hour within the stable region smaller based on the asymmetric demand pattern than the maximum stable demand per hour with regard to different fleet sizes based on the symmetric demand pattern. Unlike previous work, this study extends the stability results to a more realistic, considering exiting passengers for the first time. In reality, passengers will leave the queue system and choose other modes of transportation if they wait too long for the SAVs. The simulation results show that the proposed SAVs' dispatch policy can still stabilise the network when considering exiting passengers with different tolerance times, without requiring a time horizon like previous study (Kang and Levin 2021). The maximum stable trips per hour are the same as the scenarios without exiting passengers.

These results could provide practical applications for SAVs. For example, SAV companies could use the fast maximum stability dispatch policy to choose the number of vehicles to operate within one city to both satisfy traveller demand and ensure lower waiting times. SAV companies can also make an informed decision to balance SAV trips per hour with vehicle fleet size to optimise operating costs based on the relationship shown in Figure 6. Furthermore, when the tolerance time increases, the average queue length of waiting passengers increases too, which forces SAV companies to provide some strategies to reduce passengers' waiting queue lengths, such as ride-sharing and off-peak travel incentive. As for the government, this research could provide information relevant to regulations on SAV fleet sizes. If current fleet size can stabilise the passenger waiting queue lengths, the government may reject company requests to increase fleet sizes.

In future work, there are many extensions, such as electric vehicle charging behaviours, ride-sharing, dynamic pricing, and dynamic rebalancing, which may affect the maximum SAVs trips per hour for a given fleet size and the queue lengths of waiting passengers.

Disclosure statement

No potential conflict of interest was reported by the author(s).

Funding

The authors gratefully acknowledge the support of the National Science Foundation, [award number 1935514] and the support of Hsiao Shaw-Lundquist Fellowship of the University of Minnesota China Center.

Data availability statements

The network information and trips datasets used by the research are open to the public and are available in the github repository: Sioux-Falls Network. The authors are very grateful to the contributor.

References

Barman, S., and M. W. Levin. 2022. "Performance Evaluation of Modified Cyclic Max-Pressure Controlled Intersections in Realistic Corridors. *Transportation Research Record* 2676 (6): 110–128. doi:10.1177/03611981211072807.

Barman, S., and M. W. Levin. 2023. "Throughput Properties and Optimal Locations for Limited Deployment of Max-Pressure Controls." *Transportation Research Part C: Emerging Technologies* 150: 104105. doi:10.1016/j.trc.2023.104105.

Becker, F., and K. W. Axhausen. 2017. "Literature Review on Surveys Investigating the Acceptance of Automated Vehicles." *Transportation* 44 (6): 1293–1306. doi:10.1007/s11116-017-9808-9.

Becker, H., F. Becker, R. Abe, S. Bekhor, P. F. Belgiawan, J. Compostella, E. Frazzoli, et al. 2020. "Impact of Vehicle Automation and Electric Propulsion on Production Costs for Mobility Services Worldwide." *Transportation Research Part A: Policy and Practice* 138: 105–126. doi:10.1016/j.tra.2020.04.021.

Boesch, P. M., F. Ciari, and K. W. Axhausen. 2016. "Autonomous Vehicle Fleet Sizes Required to Serve Different Levels of Demand." *Transportation Research Record* 2542 (1): 111–119. doi:10.3141/2542-13.

Boewing, F., M. Schiffer, M. Salazar, and M. Pavone. 2020. "A Vehicle Coordination and Charge Scheduling Algorithm for Electric Autonomous Mobility-on-Demand Systems." In *2020 American Control Conference (ACC)*, 248–255. IEEE.

Chen, R., J. Hu, M. W. Levin, and D. Rey. 2020. "Stability-Based Analysis of Autonomous Intersection Management with Pedestrians." *Transportation Research Part C: Emerging Technologies* 114: 463–483. doi:10.1016/j.trc.2020.01.016.

Chen, T. D., and K. M. Kockelman. 2016. "Management of a Shared Autonomous Electric Vehicle Fleet: Implications of Pricing Schemes." *Transportation Research Record* 2572 (1): 37–46. doi:10.3141/2572-05.

Chen, T. D., K. M. Kockelman, and J. P. Hanna. 2016. "Operations of a Shared, Autonomous, Electric Vehicle Fleet: Implications of Vehicle & Charging Infrastructure Decisions." *Transportation Research Part A: Policy and Practice* 94: 243–254. doi:10.1016/j.tra.2016.08.020.

Fagnant, D. J., and K. M. Kockelman. 2014. "The Travel and Environmental Implications of Shared Autonomous Vehicles, Using Agent-based Model Scenarios." *Transportation Research Part C: Emerging Technologies* 40: 1–13. doi:10.1016/j.trc.2013.12.001.

Fagnant, D. J., and K. Kockelman. 2015. "Preparing a Nation for Autonomous Vehicles: Opportunities, Barriers and Policy Recommendations." *Transportation Research Part A: Policy and Practice* 77: 167–181. doi:10.1016/j.tra.2015.04.003.

Fagnant, D. J., and K. M. Kockelman. 2018. "Dynamic Ride-Sharing and Fleet Sizing for a System of Shared Autonomous Vehicles in Austin, Texas." *Transportation* 45 (1): 143–158. doi:10.1007/s11116-016-9729-z.

Fagnant, D. J., K. M. Kockelman, and P. Bansal. 2015. "Operations of Shared Autonomous Vehicle Fleet for Austin, Texas, Market." *Transportation Research Record* 2563 (1): 98–106. doi:10.3141/2536-12.

Farhan, J., and T. D. Chen. 2018. "Impact of Ridesharing on Operational Efficiency of Shared Autonomous Electric Vehicle Fleet." Technical Report.

Ge, Q., K. Han, and X. Liu. 2021. "Matching and Routing for Shared Autonomous Vehicles in Congestible Network." *Transportation Research Part E: Logistics and Transportation Review* 156: 102513. doi:10.1016/j.tre.2021.102513.

Golbabaei, F., T. Yigitcanlar, and J. Bunker. 2020. "The Role of Shared Autonomous Vehicle Systems in Delivering Smart Urban Mobility: A Systematic Review of the Literature." *International Journal of Sustainable Transportation* 15 (10): 731–748. doi:10.1080/15568318.2020.1798571.

Greenblatt, J. B., and S. Saxena. 2015. "Autonomous Taxis Could Greatly Reduce Greenhouse-Gas Emissions of US Light-Duty Vehicles." *Nature Climate Change* 5 (9): 860–863. doi:10.1038/nclimate2685.

Guo, H., Y. Chen, and Y. Liu. 2022. "Shared Autonomous Vehicle Management Considering Competition with Human-Driven Private Vehicles." *Transportation Research Part C: Emerging Technologies* 136: 103547. doi:10.1016/j.trc.2021.103547.

Gurumurthy, K. M., and K. M. Kockelman. 2020. "Modeling Americans' Autonomous Vehicle Preferences: A Focus on Dynamic Ride-Sharing, Privacy & Long-Distance Mode Choices." *Technological Forecasting and Social Change* 150: 119792. doi:10.1016/j.techfore.2019.119792.

Gurumurthy, K. M., K. M. Kockelman, and M. D. Simoni. 2019. "Benefits and Costs of Ride-Sharing in Shared Automated Vehicles Across Austin, Texas: Opportunities for Congestion Pricing." *Transportation Research Record* 2673 (6): 548–556. doi:10.1177/0361198119850785.

Gusfield, D., and R. W. Irving. 1989. *The Stable Marriage Problem: Structure and Algorithms*. Cambridge, MA: MIT Press.

Hörl, S., F. Becker, and K. W. Axhausen. 2021. "Simulation of Price, Customer Behaviour and System Impact for a Cost-Covering Automated Taxi System in Zurich." *Transportation Research Part C: Emerging Technologies* 123: 102974. doi:10.1016/j.trc.2021.102974.

Hörl, S., C. Ruch, F. Becker, E. Frazzoli, and K. W. Axhausen. 2019. "Fleet Operational Policies for Automated Mobility: A Simulation Assessment for Zurich." *Transportation Research Part C: Emerging Technologies* 102: 20–31. doi:10.1016/j.trc.2019.02.020.

Hanna, J. P., M. Albert, D. Chen, and P. Stone. 2016. "Minimum Cost Matching for Autonomous Carsharing." *IFAC-PapersOnLine* 49 (15): 254–259. doi:10.1016/j.ifacol.2016.07.757.

Huang, Y., K. M. Kockelman, and V. Garikapati. 2022. "Shared Automated Vehicle Fleet Operations for First-mile Last-Mile Transit Connections with Dynamic Pooling." *Computers, Environment and Urban Systems* 92: 101730. doi:10.1016/j.compenvurbsys.2021.101730.

Hyland, M. F., and H. S. Mahmassani. 2017. "Taxonomy of Shared Autonomous Vehicle Fleet Management Problems to Inform Future Transportation Mobility." *Transportation Research Record* 2653 (1): 26–34. doi:10.3141/2653-04.

Hyland, M., and H. S. Mahmassani. 2018. "Dynamic Autonomous Vehicle Fleet Operations: Optimization-Based Strategies to Assign AVs to Immediate Traveler Demand Requests." *Transportation Research Part C: Emerging Technologies* 92: 278–297. doi:10.1016/j.trc.2018.05.003.

Hyland, M., and H. S. Mahmassani. 2020. "Operational Benefits and Challenges of Shared-Ride Automated Mobility-on-Demand Services." *Transportation Research Part A: Policy and Practice* 134: 251–270. doi:10.1016/j.tra.2020.02.017.

Kang, D., and M. W. Levin. 2021. "Maximum-Stability Dispatch Policy for Shared Autonomous Vehicles." *Transportation Research Part B: Methodological* 148: 132–151. doi:10.1016/j.trb.2021.04.011.

Ke, Z., Z. Li, Z. Cao, and P. Liu. 2020. "Enhancing Transferability of Deep Reinforcement Learning-Based Variable Speed Limit Control Using Transfer Learning." *IEEE Transactions on Intelligent Transportation Systems* 22 (7): 4684–4695. doi:10.1109/TITS.2020.2990598.

Khan, N. A., and M. Habib. 2023. "Microsimulation of Mobility Assignment within an Activity-Based Travel Demand Forecasting Model. *Transportmetrica A: Transport Science* 19 (2): 1983664. doi:10.1080/23249935.2021.1983664.

Levin, M. W.. 2022. "A General Maximum-Stability Dispatch Policy for Shared Autonomous Vehicle Dispatch with an Analytical Characterization of the Maximum Throughput." *Transportation Research Part B: Methodological* 163: 258–280. doi:10.1016/j.trb.2022.07.003.

Levin, M. W., J. Hu, and M. Odell. 2020. "Max-Pressure Signal Control with Cyclical Phase Structure." *Transportation Research Part C: Emerging Technologies* 120: 102828. doi:10.1016/j.trc.2020.102828.

Li, L., T. Pantelidis, J. Y. Chow, and S. E. Jabari. 2021. "A Real-Time Dispatching Strategy for Shared Automated Electric Vehicles with Performance Guarantees." *Transportation Research Part E: Logistics and Transportation Review* 152: 102392. doi:10.1016/j.tre.2021.102392.

Liang, M., Y. Chao, Y. Tu, and T. Xu. 2023. "Vehicle Pollutant Dispersion in the Urban Atmospheric Environment: A Review of Mechanism, Modeling, and Application." *Atmosphere* 14 (2): 279. doi:10.3390/atmos14020279.

Liu, Y., F. Wu, C. Lyu, S. Li, J. Ye, and X. Qu. 2022. "Deep Dispatching: A Deep Reinforcement Learning Approach for Vehicle Dispatching on Online Ride-Hailing Platform." *Transportation Research Part E: Logistics and Transportation Review* 161: 102694. doi:10.1016/j.tre.2022.102694.

Loeb, B., and K. M. Kockelman. 2019. "Fleet Performance and Cost Evaluation of a Shared Autonomous Electric Vehicle (SAEV) Fleet: A Case Study for Austin, Texas." *Transportation Research Part A: Policy and Practice* 121: 374–385. doi:10.1016/j.tra.2019.01.025.

Loeb, B., K. M. Kockelman, and J. Liu. 2018. "Shared Autonomous Electric Vehicle (SAEV) Operations Across the Austin, Texas Network with Charging Infrastructure Decisions." *Transportation Research Part C: Emerging Technologies* 89: 222–233. doi:10.1016/j.trc.2018.01.019.

Lokhandwala, M., and H. Cai. 2018. "Dynamic Ride Sharing Using Traditional Taxis and Shared Autonomous Taxis: A Case Study of Nyc." *Transportation Research Part C: Emerging Technologies* 97: 45–60. doi:10.1016/j.trc.2018.10.007.

Ma, K., H. Wang, and T. Ruan. 2021. "Analysis of Road Capacity and Pollutant Emissions: Impacts of Connected and Automated Vehicle Platoons on Traffic Flow." *Physica A: Statistical Mechanics and Its Applications* 583: 126301. doi:10.1016/j.physa.2021.126301.

Ma, K., H. Wang, Z. Zuo, Y. Hou, X. Li, and R. Jiang. 2022. "String Stability of Automated Vehicles Based on Experimental Analysis of Feedback Delay and Parasitic Lag." *Transportation Research Part C: Emerging Technologies* 145: 103927. doi:10.1016/j.trc.2022.103927.

Martinez, L. M., and J. M. Viegas. 2017. "Assessing the Impacts of Deploying a Shared Self-Driving Urban Mobility System: An Agent-Based Model Applied to the City of Lisbon, Portugal." *International Journal of Transportation Science and Technology* 6 (1): 13–27. doi:10.1016/j.ijtst.2017.05.005.

Mourad, A., J. Puchinger, and C. Chu. 2019. "A Survey of Models and Algorithms for Optimizing Shared Mobility." *Transportation Research Part B: Methodological* 123: 323–346. doi:10.1016/j.trb.2019.02.003.

Narayanan, S., E. Chaniotakis, and C. Antoniou. 2020. "Shared Autonomous Vehicle Services: A Comprehensive Review." *Transportation Research Part C: Emerging Technologies* 111: 255–293. doi:10.1016/j.trc.2019.12.008.

Poulhès, A., and J. Berrada. 2020. "Single Vehicle Network Versus Dispatcher: User Assignment in an Agent-Based Model." *Transportmetrica A: Transport Science* 16 (2): 270–292. doi:10.1080/23249935.2019.1570383.

Santos, G. G. D., and G. H. de Almeida Correia. 2021. "A Flow-Based Integer Programming Approach to Design an Interurban Shared Automated Vehicle System and Assess Its Financial Viability." *Transportation Research Part C: Emerging Technologies* 128: 103092. doi:10.1016/j.trc.2021.103092.

Sun, X., and Y. Yin. 2018. "A Simulation Study on Max Pressure Control of Signalized Intersections." *Transportation Research Record* 2672 (18): 117–127. doi:10.1177/0361198118786840.

Tassiulas, L., and A. Ephremides. 1990. "Stability Properties of Constrained Queueing Systems and Scheduling Policies for Maximum Throughput in Multihop Radio Networks." In *29th IEEE Conference on Decision and Control*, 2130–2132. IEEE.

Teoh, E. R., and D. G. Kidd. 2017. "Rage Against the Machine? Google's Self-Driving Cars Versus Human Drivers." *Journal of Safety Research* 63: 57–60. doi:10.1016/j.jsr.2017.08.008.

Tu, Y., W. Wang, Y. Li, C. Xu, T. Xu, and X. Li. 2019. "Longitudinal Safety Impacts of Cooperative Adaptive Cruise Control Vehicle's Degradation." *Journal of Safety Research* 69: 177–192. doi:10.1016/j.jsr.2019.03.002.

Varaiya, P.. 2013. "Max Pressure Control of a Network of Signalized Intersections." *Transportation Research Part C: Emerging Technologies* 36: 177–195. doi:10.1016/j.trc.2013.08.014.

Vazifeh, M. M., P. Santi, G. Resta, S. H. Strogatz, and C. Ratti. 2018. "Addressing the Minimum Fleet Problem in on-Demand Urban Mobility." *Nature* 557 (7706): 534–538. doi:10.1038/s41586-018-0095-1.

Wang, X., N. Agatz, and A. Erera. 2018. "Stable Matching for Dynamic Ride-Sharing Systems." *Transportation Science* 52 (4): 850–867. doi:10.1287/trsc.2017.0768.

Wang, H., and H. Yang. 2019. "Ridesourcing Systems: A Framework and Review." *Transportation Research Part B: Methodological* 129: 122–155. doi:10.1016/j.trb.2019.07.009.

Xu, T., S. Barman, M. W. Levin, R. Chen, and T. Li. 2022. "Integrating Public Transit Signal Priority Into Max-pressure Signal Control: Methodology and Simulation Study on a Downtown Network." *Transportation Research Part C: Emerging Technologies* 138: 103614. doi:10.1016/j.trc.2022.103614.

Xu, T., Y. Bika, and M. Levin. n.d. a. "An Approximate Position-Weighted Back-Pressure Traffic Signal Control Policy for Traffic Networks." Available at SSRN 4186584.

Xu, T., Y. Bika, and M. Levin. n.d. b. "Ped-MP: A Pedestrian-Friendly Max-Pressure Signal Control Policy for City Networks." Available at SSRN 4330375.

Yang, M., Z. Li, Z. Ke, and M. Li. 2019. "A Deep Reinforcement Learning-Based Ramp Metering Control Framework for Improving Traffic Operation at Freeway Weaving Sections." In *Proceedings of the Transportation Research Board 98th Annual Meeting*, Washington, DC, USA, 13–17.

Yu, X., J. Chen, P. Kumar, A. Khani, and H. Mao. 2022. "An Integrated Optimisation Framework for Locating Depots in Shared Autonomous Vehicle Systems." *Transportmetrica A: Transport Science*, 1–39. doi:10.1080/23249935.2022.2152299.

Zhang, T. Z., and T. D. Chen. 2020. "Smart Charging Management for Shared Autonomous Electric Vehicle Fleets: A Puget Sound Case Study." *Transportation Research Part D: Transport and Environment* 78: 102184. doi:10.1016/j.trd.2019.11.013.

Zhang, W., and S. Guhathakurta. 2017. "Parking Spaces in the Age of Shared Autonomous Vehicles: How Much Parking Will We Need and Where?" *Transportation Research Record* 2651 (1): 80–91. doi:10.3141/2651-09.

Zhang, R., and M. Pavone. 2016. "Control of Robotic Mobility-on-Demand Systems: A Queueing-Theoretical Perspective." *The International Journal of Robotics Research* 35 (1-3): 186–203. doi:10.1177/0278364915581863.

Zhang, R., F. Rossi, and M. Pavone. 2016. "Model Predictive Control of Autonomous Mobility-on-Demand Systems." In *2016 IEEE International Conference on Robotics and Automation (ICRA)*, 1382–1389. IEEE.

Zhou, L., T. Ruan, K. Ma, C. Dong, and H. Wang. 2021. "Impact of Cav Platoon Management on Traffic Flow Considering Degradation of Control Mode." *Physica A: Statistical Mechanics and Its Applications* 581: 126193. doi:10.1016/j.physa.2021.126193.